WHITE PAPER

November 2024, Revision V1.15.

EWA sensors for Condition Monitoring

on

Rotating Machinery

www.ewasensors.com

Prepared by Eva Kühne, founder

Preword

The condition monitoring and predictive maintenance communities are a very active research and development area, with +150 IIoT solutions being offered for industrial applications. Common denominators are powerful cloud AI and ML capabilities combined with non-realtime data access.

The EWA sensor is designed with a different mindset, and the purpose of the current Whitepaper is to address the following four differentiators:

1. Machine condition monitoring can be done without Artificial Intelligence (AI) and Machine Learning (ML) algorithms because the main part of all machine failure modes is already well described by ISO-18436. Knowing the fault signatures and understanding the physics of the machine have prone the way to developing an autonomous sensor platform like the EWA sensor.

   In general, when physical relations are known, there is no need for AI modeling - like the FFT algorithm for frequency analysis, it will outperform any AI system regarding precision and speed - anytime. But for unknown and complicated physical relations, AI and ML might be the only solutions possible.

   The EWA sensor can with benefit be used as a preprocessing unit for larger AI/ML cloud-based Condition Monitoring Solutions (CMS), as the sensor provides access to both high-level performance parameters and low-level raw data.

2. Combining *Vibration Signature Analysis* and *Motor Current Signature Analysis* will provide the insight and robustness required for industrial applications. Sensor solutions based on vibration measurement only, are very sensitive to contributions from surrounding operating machinery.

3. Plug and play – no setup is required for the EWA Sensor.

   The orientation of the installation (horizontal/vertical) is auto-detected, the pole pair size of the motor (1,2 or 3 pole pairs) is auto-detected, bearing faults are detected without requiring the bearing type number, motor rotation speed and rotation direction is auto-detected, fixed valued alarm levels are not needed, as Machine Health levels are adaptive tracking machine aging and wear.

4. As an edge device with real-time analytics of 3D vibration signals and 3D magnetic signals, the EWA Sensor performs a complete analysis of all parameters every second. This high-resolution parameter set is used internal by the Machine Health center for baseline tracking and can be accessed randomly by customers using Modbus interface.

The EWA sensor is offered as a retrofit sensor solution, but the autonomous edge platform can easily be built into machines from factory. This will leverage machines like pumps from ”just” being actuators to become actually intelligent devices, and this is expected to become an important business differentiator for machine manufacturers in the near future.

Table of content

1. Motivation

Rotation machinery has been the driving horse behind the Fourth Industrial Revolution (Industry 4.0), with focus on system uptime and process optimization. Critical machines have always been nursed daily by machine service operators to ensure proper lubrication, alignment, and general working conditions.

Machine maintenance has been based on experience of the service staff, using simple tools like "Engine Defect Finder", which is a stethoscope-like instrument used for the early detection of bearing and machine damage – see the picture of top of this section (”Original Maschinen und Motoren Defekt-Sucher” from the company Apparatebau C. Richter, 1920). This manual machine inspection tool was both expensive and difficult to scale, as the maintenance expertise was built up over many years by individual machine service operators.

100 years after the development of the Engine Defect Finder instrument, machine inspection has been taken over by scalable IoT solutions, offering a wide portfolio of condition monitoring solutions. Today, machine condition monitoring is a range of techniques and technologies used to monitor the condition and performance of various machine parts within the machine.

These IoT solutions primarily focus on extracting parameters to identifying significant changes (abnormalities) that may indicate impending failures, as the collected data is analyzed to identify patterns or trends that can indicate wear, damage, or other machine related issues. This offering is categorized as **Predictive Maintenance** and serves to increase system uptime and reduce unnecessary maintenance expenses. But predictive maintenance is only one part of the complete picture, that a condition monitoring sensor can provide for the end user. Fortunately - the main part of the machine park will run for years without any breakdown, so predictive maintenance becomes like an insurance (fear management) - you don't want to use it, and you don't want to live without it. The second part of the complete picture is **Daily Operation Parameters**. This offering provides valuable insights into machine operation and means for process optimization - just to name three examples:

- *Energy optimization:* saving energy by reducing motor rpm without harming or damaging machine components. E.g. the gear box in a mixer will wear faster, if the oil is not rated to low speed operation, which can be observed from the Gear Mesh Frequency vibration level.
- *Resonance detection:* observing vibration level for different motor rpm.
- *Process control:* avoid cavitation in some process facilities by reducing rpm, adjusting air diffusers in a treatment plant by observing the mixer 3D vibration level. Too little air and the chemistry will not work, but too much air will go behind the impeller, and the non-uniform load will break the mixer of the tower, leading to a total breakdown.

The third part of the complete picture is EWA sensor data to support **Artificial Intelligence and Machine Learning**. Continuous streaming of multi-dimensional, high resolution raw sensor data to a cloud platform is neither a green technology nor technical feasible. Raw data stays at the source and information are communicated to the cloud, where new insight is created by datamining across many installations and data sources. As a preprocessing frontend for AI and ML platforms, the EWA sensor data can boost the performance significantly.

By exploiting all three parts of the condition monitoring picture, the return of investment will be high compared to other type of investments, because it has a 3D impact on the information flow in a production facility. This is illustrated in the following ***Return of Investment Tree***, see Figure 1.

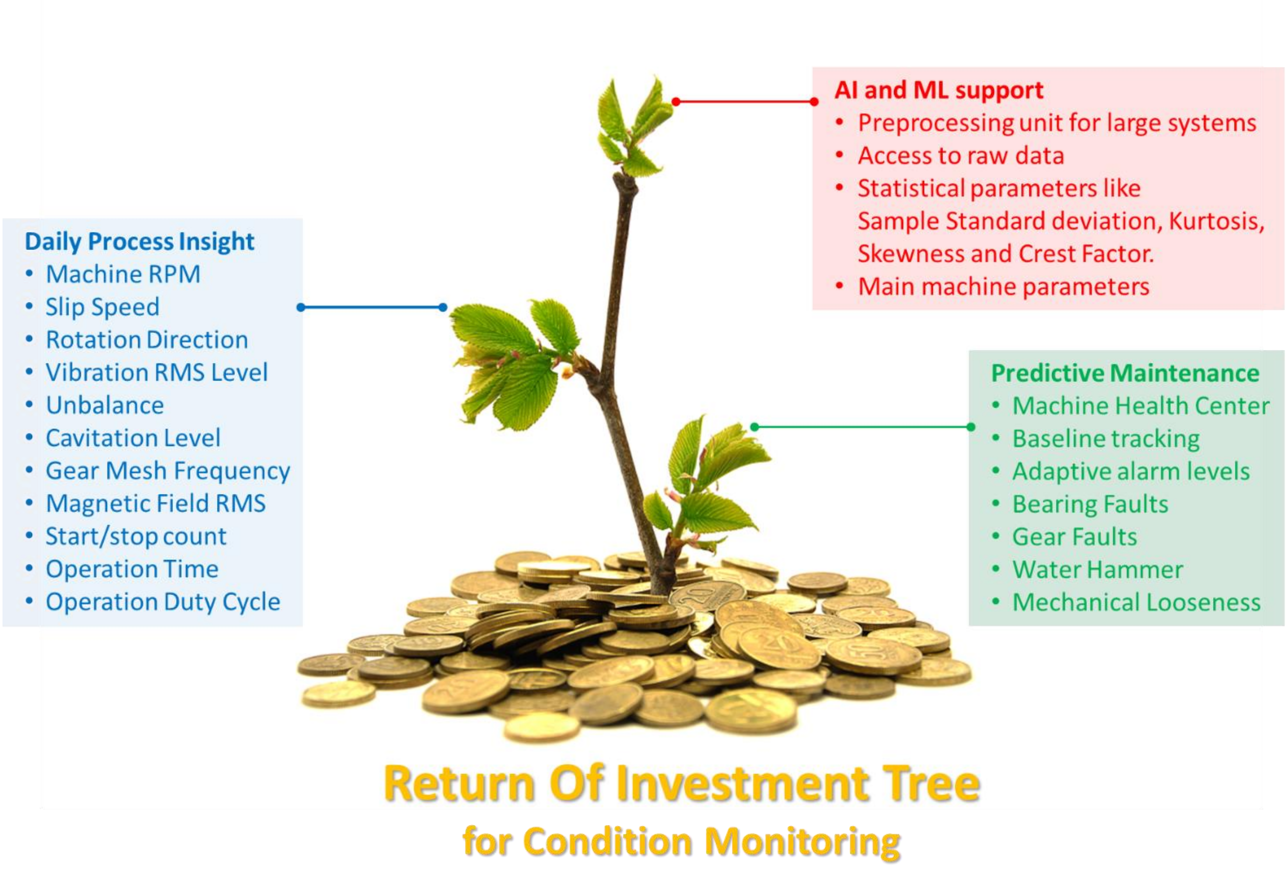

Figure 1: The EWA platform creates high-quality sensor data and insights for 1) Predictive Maintenance, 2) within Daily Process Insights and 3) for AI and ML support.

2. Predictive Maintenance

Regarding predictive maintenance a quote from the Nobel prize-winning Quantum physicist Niels Bohr states: "It is difficult to make predictions, especially about the future".

Forecasting can be a dangerous art, as it easily breakdown due to unexpected events that can't be incorporated into a model. To optimize production time and minimize maintenance cost, a shift from normal prescriptive maintenance (regular time intervals) to predictive maintenance has emerged. It is important to align expectations, as predictive maintenance is not the same as the ability to foresee the future. Based on current condition monitoring values, and the trend leading up to this, a qualified estimate can be made for the coming measurements. But there is no black magic involved in predictive maintenance.

Predictive maintenance is not a time prediction (as e.g. 3641 hours to break down), but more an event prediction, like the development of a bearing damage. In isolated applications with known constant operation condition, models for time predictions can provide reasonable time estimation before breakdown. But in real life applications, where nothing is constant and much is unknown, breakdown time prediction will be with high uncertainty and of little practical value.

3. The EWA Platform

A platform for condition monitoring must be build much more robust than the machinery it is monitoring and protecting. It must withstand impact from many sources like vibration forces, high pressure cleaning, tough handling, water and chemical liquids, pressure from submerged installations etc. The parameter robustness must be ensured using a foundation of multiple signal sources. This makes the design of a platform for condition monitoring a technical challenging task, and the EWA Platform is created with this mindset.

Machine insight is obtained with real-time analytics of sensor signals, that capture the essential operation of the machine. Many IoT solutions are blinded 99% of the time, as they are only measuring on an hourly basis to save battery power, and therefore often miss the big picture in many applications. The tradeoff between a battery power wireless platform and a powered wired platform comes down to a choice between flexibility and data insight. The EWA platform is designed for data insight, a wired edge processing platform where all algorithms are updated every second - providing a time resolution 3600 times larger than most IoT platforms.

The quality of condition monitoring parameters is depending on two things – the algorithms and the sensor signals. The purpose of the sensor signals is to capture the essential operation of the machine, and robustness comes by using a multi sensor approach. Traditionally, vibration analysis has been the primary tool for route-based maintenance, but for autonomous CMS systems, vibration analyze often comes in short to be insufficient. The required robustness for autonomous CMS systems is obtained by combining two fundamental signal domains - vibration and magnetic. The synergy is very strong, and it counteract many of the limitation seen in “vibration-only” solutions.

Quality sensor signals require quality sensor components, and they are costly:

- The EWA vibration signals are measured in 3D, using three individual MEMS sensors (ADXL1002) from Analog Devices. They are analog with a linear frequency response range from dc to 11 kHz, a resonant frequency of 21 kHz and a noise floor of 25 µg/√Hz. To this date, ADXL1002 is the best (and most costly) accelerometer for embedded applications.
- The magnetic signal is measured using a 3D coil. The benefit of using coils from Hall sensors are higher sensitivity, low noise, but at the expense of a frequency dependent response.
- The temperature is measured with an I^2C TMP1075 temperature sensor, with a temperature resolution of 0.0625°C and a temperature accuracy of ±0.25°C, in the range from −55°C to +125°C.

All sensor signals are sampled and processed by an ARM Cortex M7 microcontroller from STMicroelectronics. The interface to the platform is both visual (4 LEDs for Power, Rotation Direction, Modbus status, and Machine Health) and through a field bus interface (Modbus RTU). The principle is illustrated in the following Figure 2:

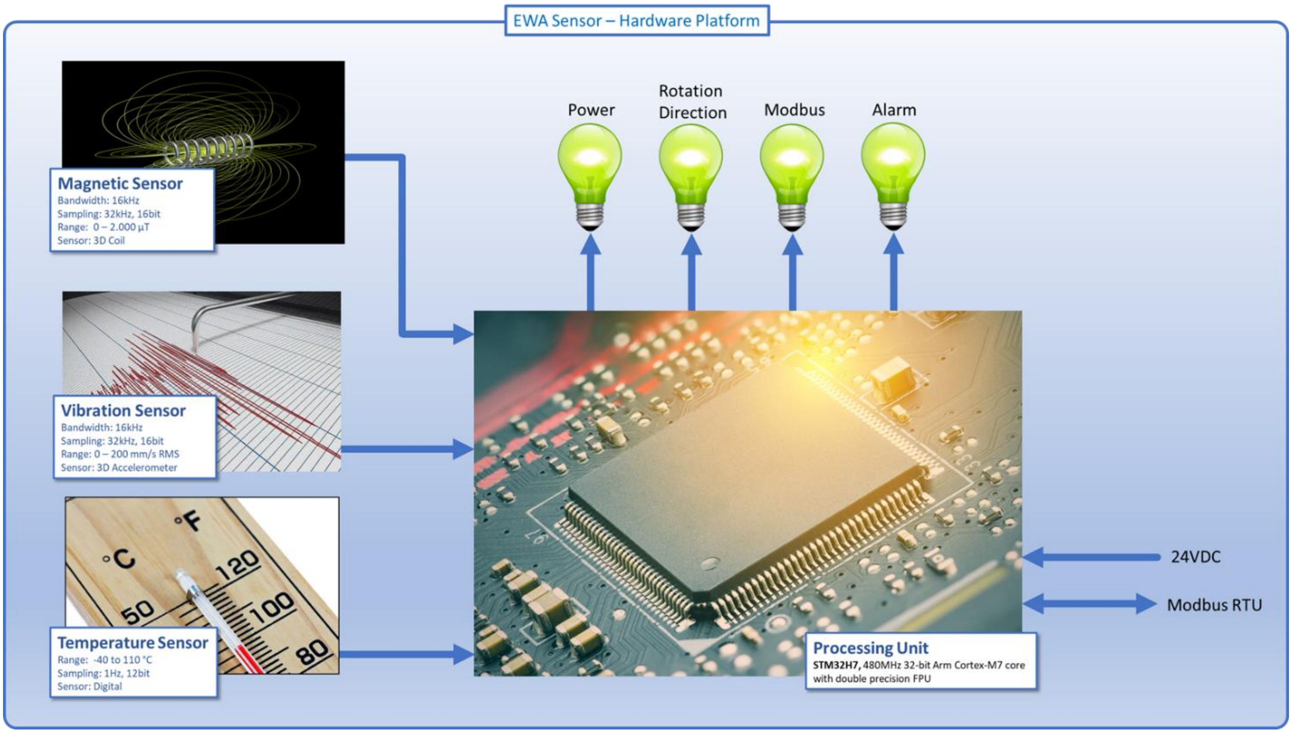

Figure 2: Schematics illustration of the EWA sensor platform. It illustrates the three sensor domains (magnetic, vibration, temperature), the ARM Cortex-M7 MCU and outputs both as visual LEDs and through Modbus RTU interface.

Some condition monitoring parameters are best measured in the vibration domain and other parameters are best measured in the magnetic domain. The overlap of parameters measurable in both domains benefit in robustness, being immune from contributions from other operating machinery.

The EWA sensor is a new solution in this context, offering unprecedented insights by combining both vibration and magnetic measurements together with edge analytics, where all parameters are recalculated every second. The key benefits of a hybrid sensor platform like the EWA sensor platform, measuring both the rotating centrifugal force in 3D and the rotating magnetic field in 3D, is selectivity and robustness. The EWA sensor calculates a long range of parameters every second and states all results in a Modbus table for customers' access.

The EWA Sensor algorithm portfolio is illustrated in the following Figure 3.

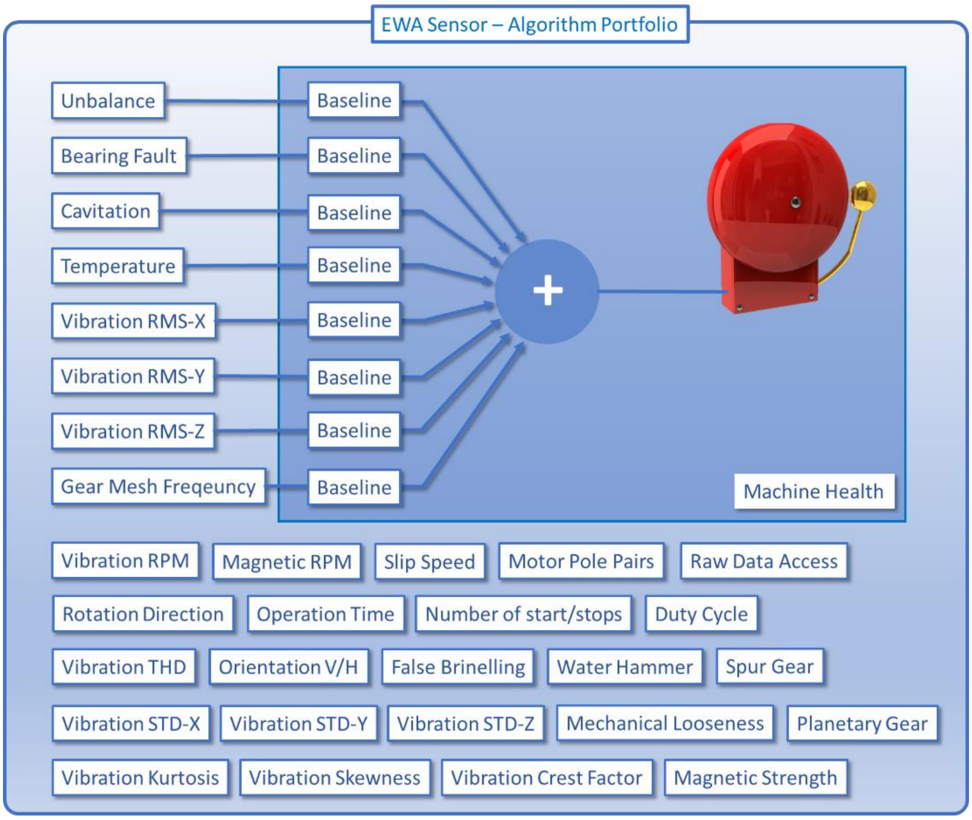

Figure 3: The EWA sensor portfolio.

Algorithms are utilizing different parts of the vibration spectra, and to optimize processing speed and spectral resolutions, the signal processing platform is designed as a multi-rate system with three different sampling rates: 32kHz (Band 1), 8kHz (Band 2) and 2kHz (Band 3).

The following Figure 4 illustrates the three bands marked in red, on top of a vibration spectra plotted in blue. The same figure also illustrates which part of the spectrum is used by the different algorithms:

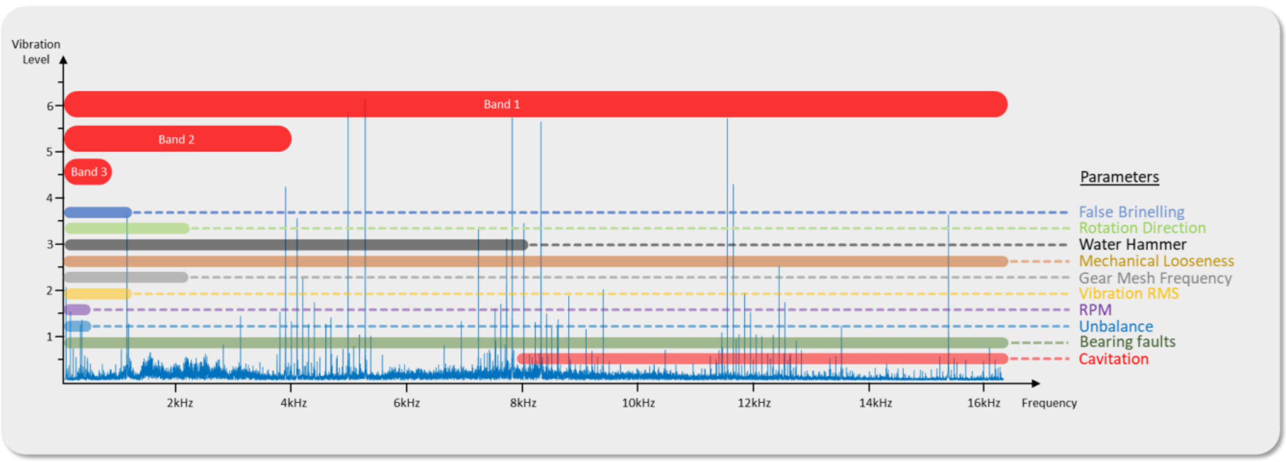

Figure 4: The EWA sensor platform works with a vibration level bandwidth of 16 kHz. The blue curve is a monitored vibration signal, where the y-axis states the actual vibration levels. On top of this figure is added, where the significant signatures for different sensor parameters are placed in the frequency spectrum (the parameters are stated on the right-hand side of the plot).

Working in a 16 kHz bandwidth has two main benefits: it is possible to detect parameters with signatures in the higher frequency band (e.g. cavitation), and it increases the fault detection parameter robustness.

Many failure modes introduce a periodic structure in the vibration signal, and a corresponding harmonic structure in the spectra. Higher bandwidth of the accelerometers will increase the number of detectable harmonic components, and thereby boost the feature gain. This is a major differentiator from low spec accelerometers often seen in many IoT devices. Accelerometers with a bandwidth of 2-3 kHz will only reproduce a finite number of harmonics, and thereby not boost the feature gain from the noise floor. One algorithm that benefit from this phenomenon is the bearing fault detection algorithm based on Cepstral Analysis.

The front of the EWA sensor contains four LED to provide basic information to the user and the walk-around service staff, see Figure 5.

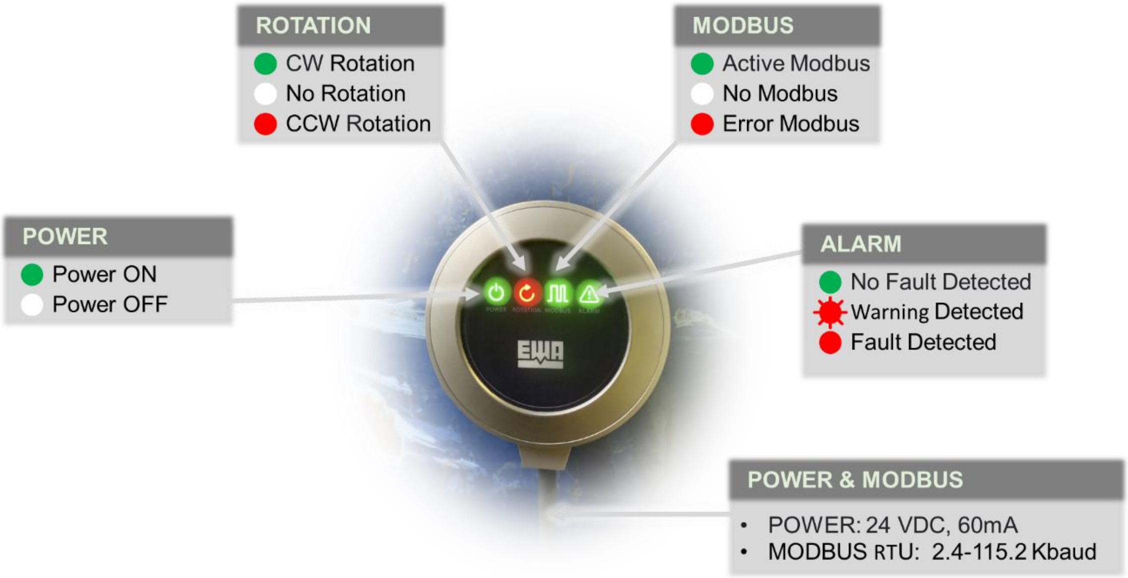

Figure 5: LED indications on EWA sensor front.

4. Submersible sensor

The mechanical design of the EWA sensor is inspired by a diving watch, to enable it to be submersible into tank environments and withstand harsh industrial applications.

The sensor house is constructed as a stainless-steel pressure capsule with O-ring gasket for both housing and cable gland. It is rated for 10 meters depth but tested with a depth of 30 meters.

Figure 6: Encapsulation testing, of the EWA sensor.

Machine Rotation Speed - RPM

5. RPM (Rotation Per Minute)

The most important question regarding rotating machinery is to confirm whether the machine is operating or not – do we have a rotation?

A lot of technology developments have emerged since machine RPM was measured using vibrating reed tachometers – a mechanical resonance design with a range of accurately calibrated reeds, tuned to selected frequencies of vibrations, indicating the speed in RPM on the meter's scale (see this section's header picture).

However, vibration on the line frequency is not a clear sign of an operating machine - it could be the operation of the machine next to you.

To determine the rotation speed and rotation direction for a machine, the EWA sensor measures both the vibration force and magnetic field using 3D sensors in both domains. By combining Vibration Signature Analysis and Motor Current Signature Analysis, a very robust measure of the machine RPM is obtained for both shaft and magnetic rotation.

RPM is a signed number, where positive RPM indicates clockwise rotation (CW) and negative RPM indicates counterclockwise (CCW) rotation. In general, rotation speed is often regarded as a fixed number, but nothing could be more misleading.

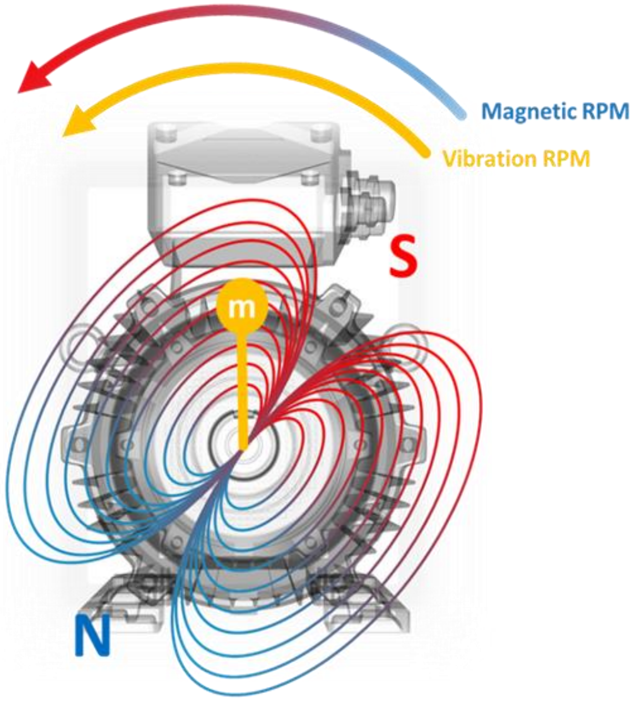

*Figure 7: A machine produces both a rotating magnetic field (**N**orth and **S**outh pole) and a rotating centripetal from unbalance **m**ass.*

Rotation speed is a time function, and the RPM fluctuation of a pump impeller contains a lot of information on the pump loading and the liquid homogeneity - this will be evidenced with the EWA sensor when the RPM is estimated with one second time resolution - as illustrated in the following recording from a wastewater pump application.

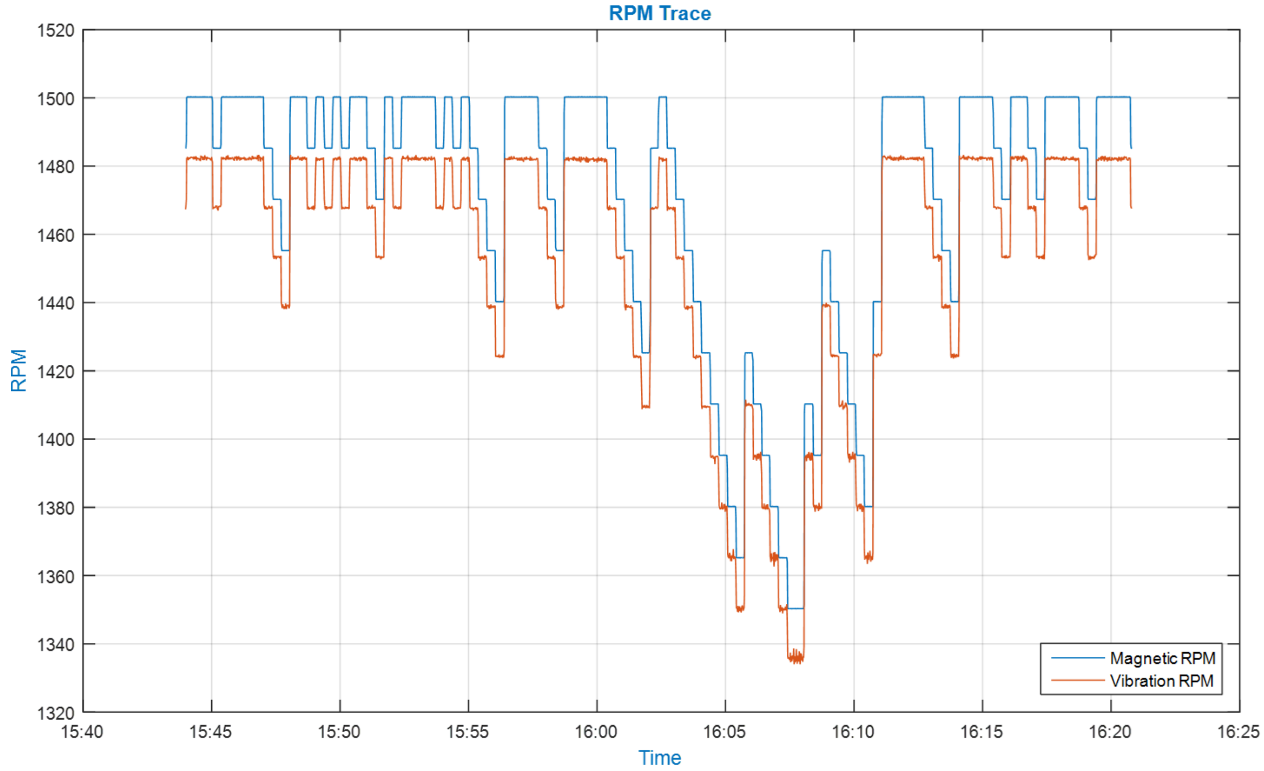

Figure 8: Measured RPM for a wastewater pump with a one second time resolution. The blue curve is the measured electrical speed (in RPM) of the magnetic field, and the orange curve is the measured mechanical rotation speed (in RPM) of the rotor shaft.

The figure illustrates the recorded Modbus data for vibration RPM (orange curve) and magnetic RPM (blue curve). The magnetic RPM is driving the vibration RPM (the shaft is the driven part). In the case of an AC motor (as we have here), the curves will be offset with the Slip Speed of the motor. The Slip Speed provides a lot of insight about the operation of the machine, and it is therefore extracted as a separate parameter – see later section. The absolute size of the Slip Speed is related to the loading of the machine, and the fluctuation of the vibration RPM is related to liquid homogeneity and pump clogging.

With a time resolution of one second, even small operation events are captured by the RPM parameter, like the short reverse rotation of a pump during startup, see Figure 9.

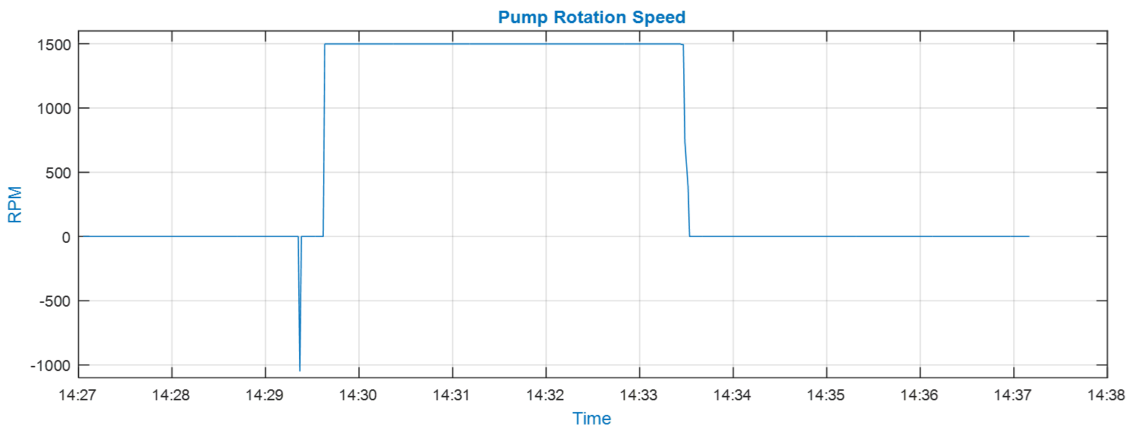

Figure 9: Measured rotation speed for a pump, with a short reverse rotation at upstart.

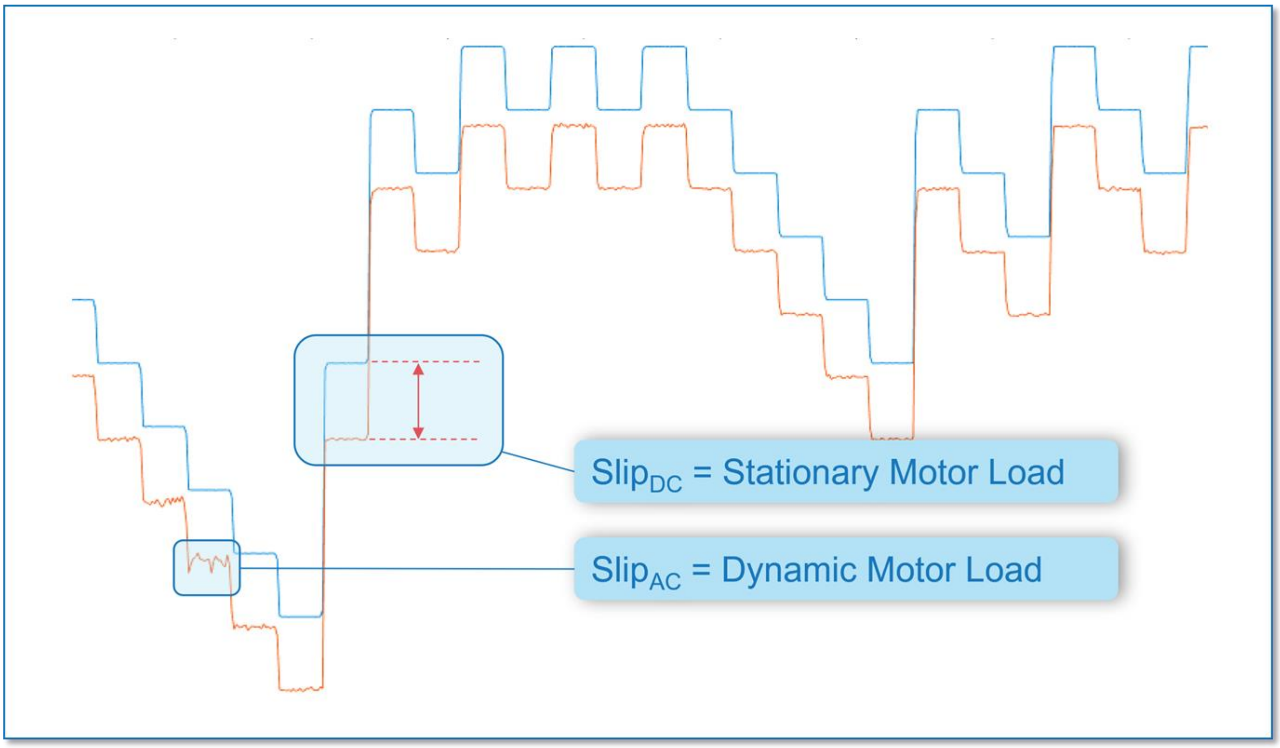

6. Slip Speed

In theory, the Slip Speed is defined as the difference between magnetic RPM and the vibration RPM.

However, this introduces some large glitches in the start/stop process, where the magnetic RPM might be 3.000 RPM and the vibration RPM is small, as the machine is ramping up. To counteract these cases, the calculated Slip Speed parameter is obtained by median filtering the RPM difference.

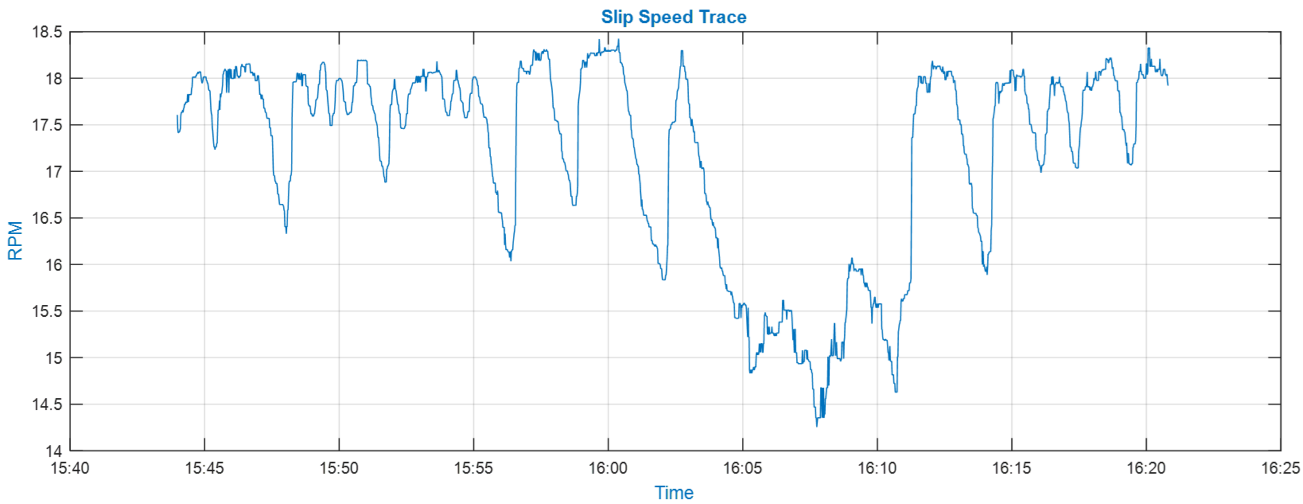

Figure 10: Measured slip speed, using a median filtering.

The Slip speed can be separated into an DC part (mean of the slip speed) and an AC part (slip speed with mean removed). The slip speed DC is a low noise version of the slip speed and are related to the loading of the motor - this parameter is stated as Slip Speed on the Modbus. The slip speed AC is the noise on the original slip speed and is related to inhomogeneous of the pumped liquid. The slip speed AC parameter can be access from the development part of the Modbus address space.

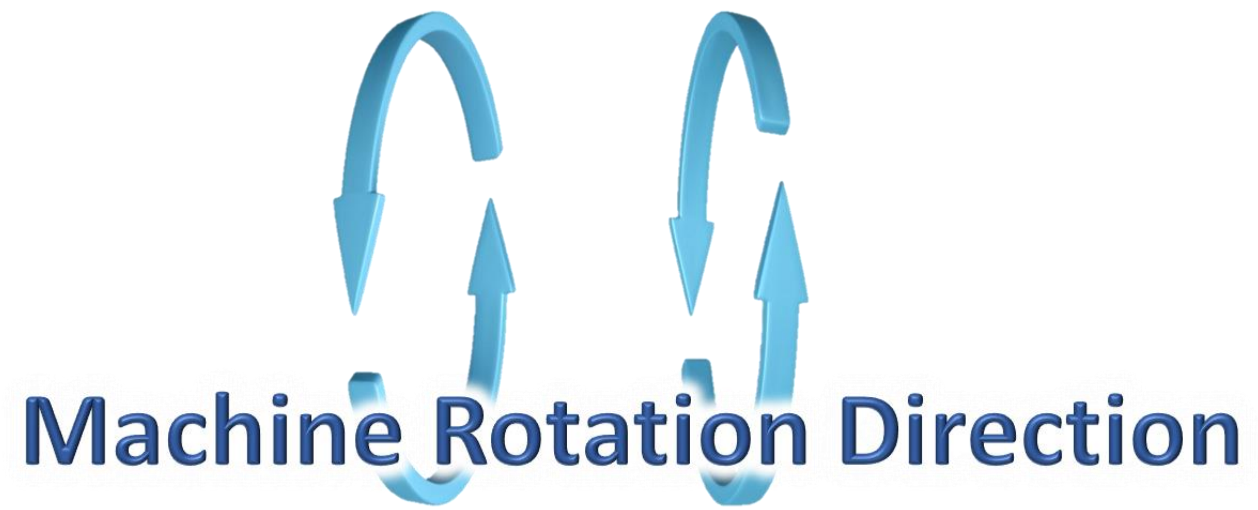

7. Rotation Direction

Rotation speed, measured in RPM, is a signed number, where positive RPM indicates clockwise rotation (CW) and negative RPM indicates counter clockwise (CCW) rotation. The sign of the RPM indicates the actual rotation direction of the motor and is measured as a separate parameter.

Rotation direction is a fundamental parameter for rotating machinery, and therefore this value is indicated on the sensor front-end with a dedicated LED: Green indicates clockwise rotation (CW), Red indicates counterclockwise (CCW) rotation, and NO LIGHT indicates no rotation (N). See Figure 11.

The rotation convention is "drive to driven", where the standing behind the motor in the drive-end define the rotation direction. If another convention is used, the definition can be reversed using a specific setup register address on the Modbus.

Rotation direction is an important parameter, as rotation direction can be mistakenly switched after a machine service, if the power cables are incorrectly reconnected by mistake. Numerous real-life cases exist with sewage pumps, that have been operating for years with wrong rotation direction, without anybody has noticed anything, other with the result of lower performance (can be reduced with up to 50-60%).

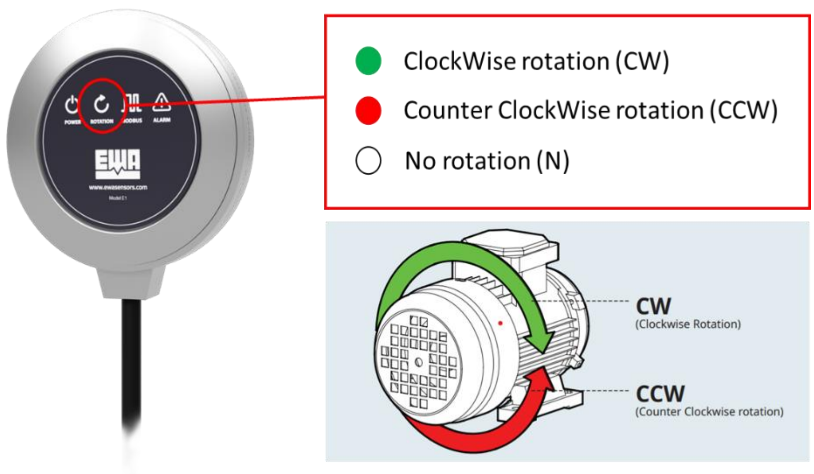

Figure 11: A LED on the sensor front indicates the actual motor rotation direction.

The Rotation Direction parameters can be accessed as a dedicated Modbus parameter, being updated every second. The Modbus parameter value 1 indicate clockwise rotation (CW), the value 2 indicates counterclockwise (CCW) rotation, and the value 0 indicate no rotation (N). See Figure 12.

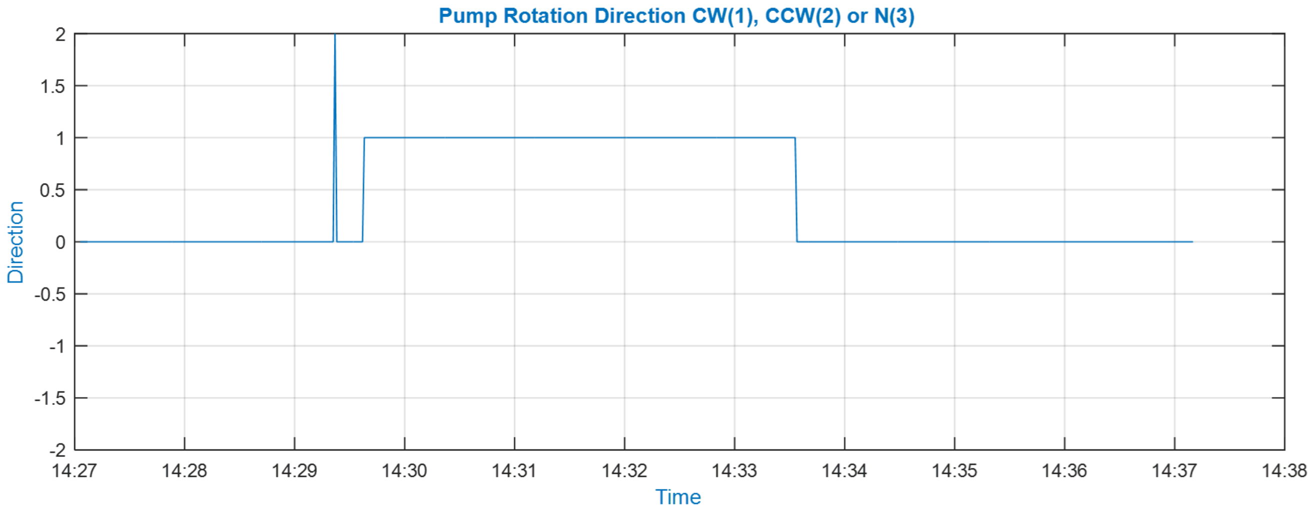

Figure 12: Monitoring of machine rotation direction.
"0" indicates "pump not running", "1" indicates "pump running clockwise", and "2" indicates "pump running counterclockwise".
Data illustrate a reverse rotation at pump startup, to avoid or minimize eventual impeller clogging.

The rotation direction algorithm has two EWA patents pending.

8. Start/Stop

One of several additional process insight parameters that can be derived from a robust RPM algorithm is the start/stop count. The Start/Stop algorithm counts the shift from zero to non-zero RPM, both as the number of start/stop events within the last 24-hour time frame and as a total accumulated count for the period since the sensor was installed.

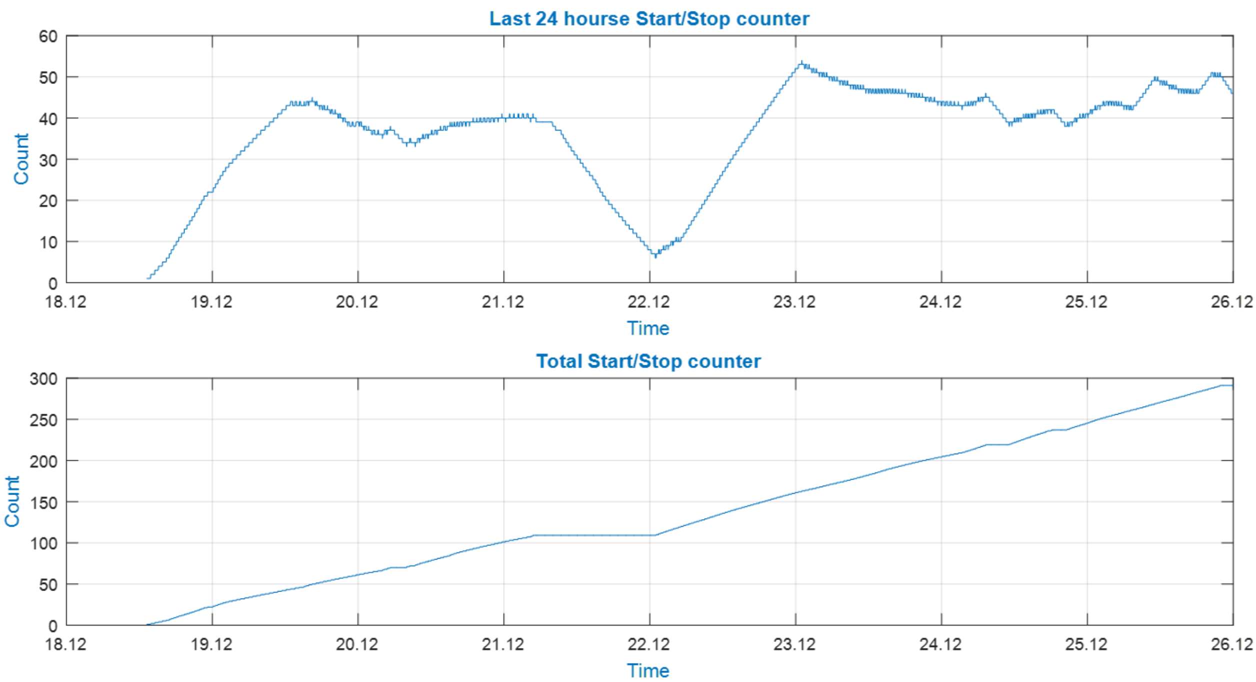

Figure 13: The upper plot illustrates start/stop counts, where each plotted value is measured for a 24-hours operation period. The lower plot illustrates the measured number of total start/stops (accumulated value), since the sensor was installed.

9. Operation Time

The operation time of the machine is another parameter derived from the RPM algorithm - measuring the operation time with a RPM larger than zero. The operation time is measured both as the operation time for the last 24-hour time frame, and as a total accumulated operation time for the machine, see Figure 14.

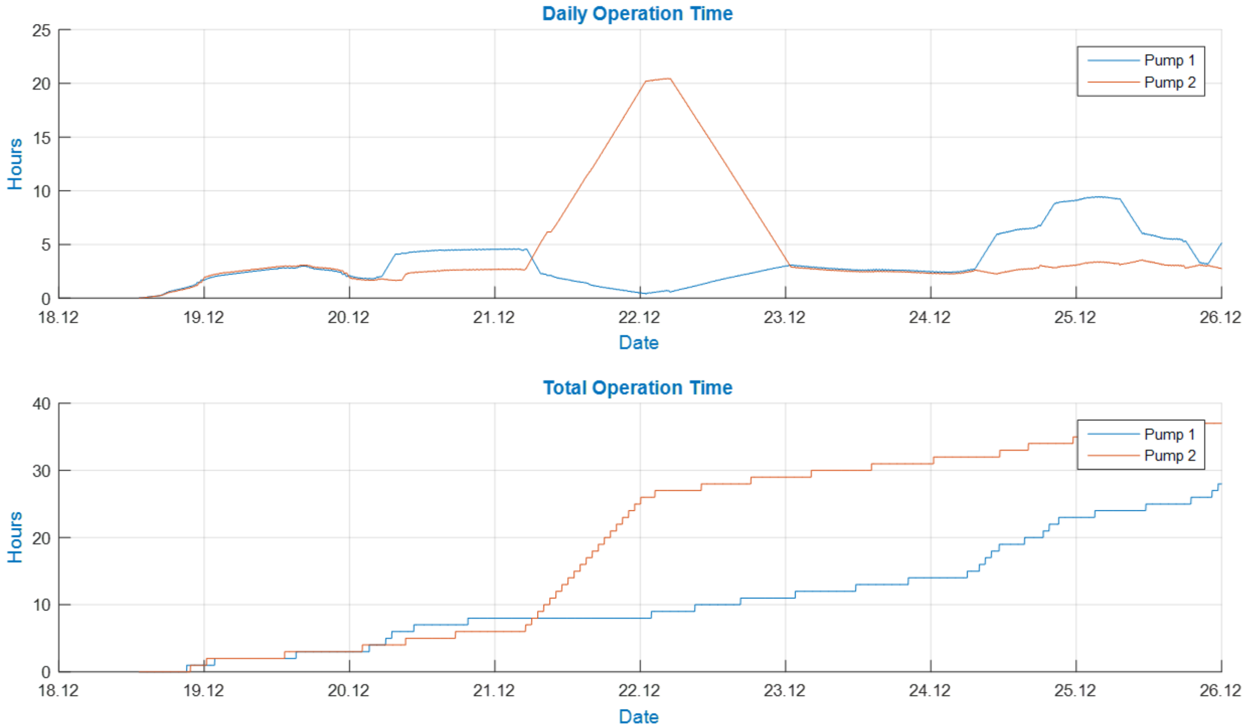

Figure 14: Upper plot illustrates the daily operation time for a period of 8 days, for two redundant pumps. The lower plot illustrates the total operation time of the two redundant pumps since the sensors were installed on the machines.

10.Unbalance

The effect from a mass unbalance in a rotating system is a centrifugal force, that is increasing with the square of the rotation speed and with the actual amount of mass unbalance.

It manifests itself in the vibration spectrum in the form of an energy component at a frequency corresponding to the rotation frequency of the shaft.

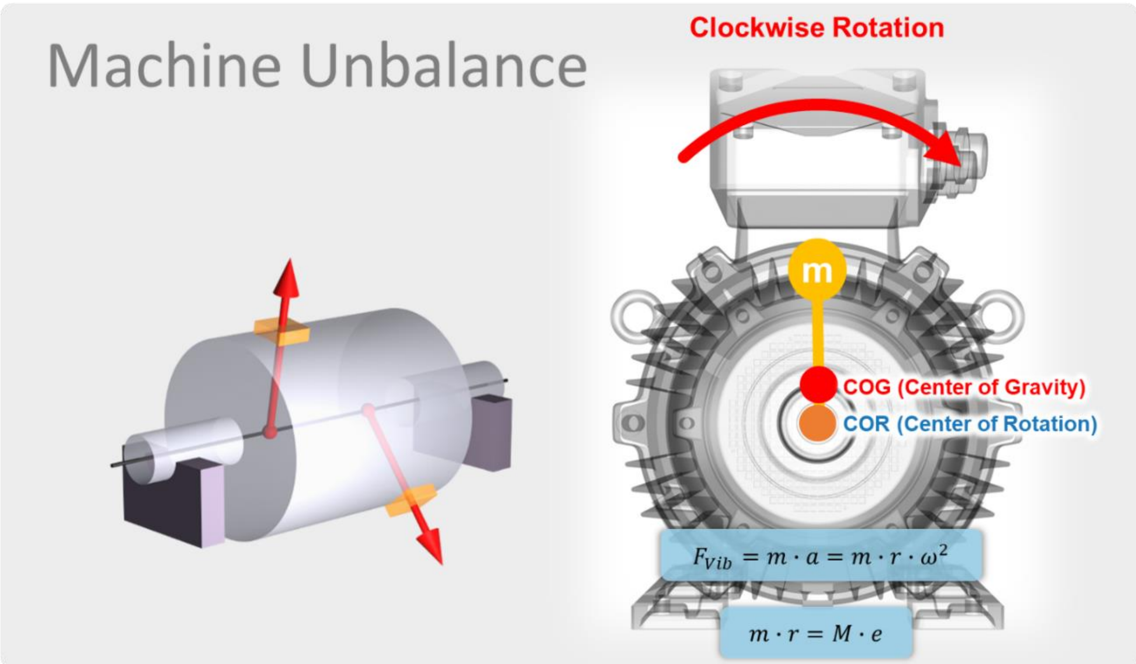

Figure 15: Illustration of unbalance mass (m) on a motor, as the center of gravity (COG) is not similar as the center of rotation (COR).

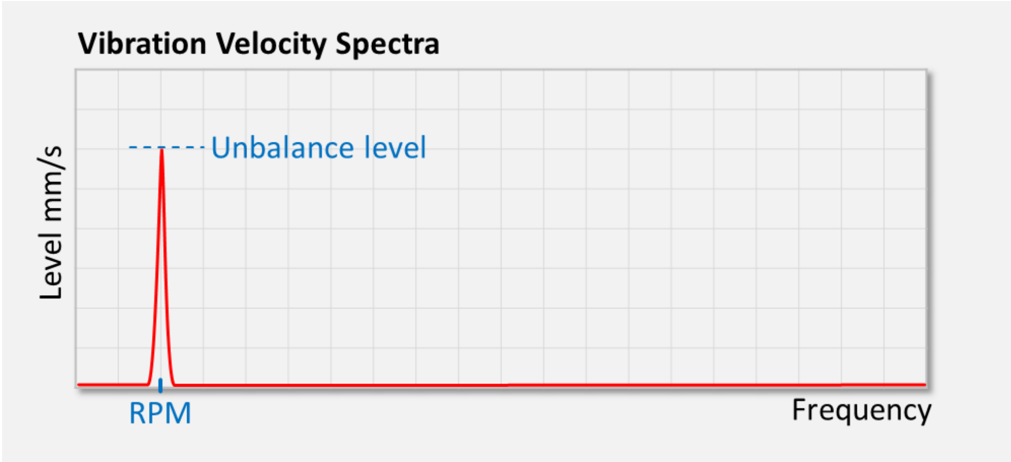

Figure 16: Measurement of the unbalance level, as the high of the 1X peak in the frequency spectrum.

The measured unbalance level depends on the actual sensor mounting position, because structural mobility might either attenuate or amplify the measured unbalance level, depending on the machine rotation frequency.

Unbalance is measured using acceleration sensor measurement (mm/s^2) and converted to velocity (mm/s), to reduce frequency dependency. Because the unbalance level is measured every second, the EWA sensor captures both short start-stops and longtime operations.

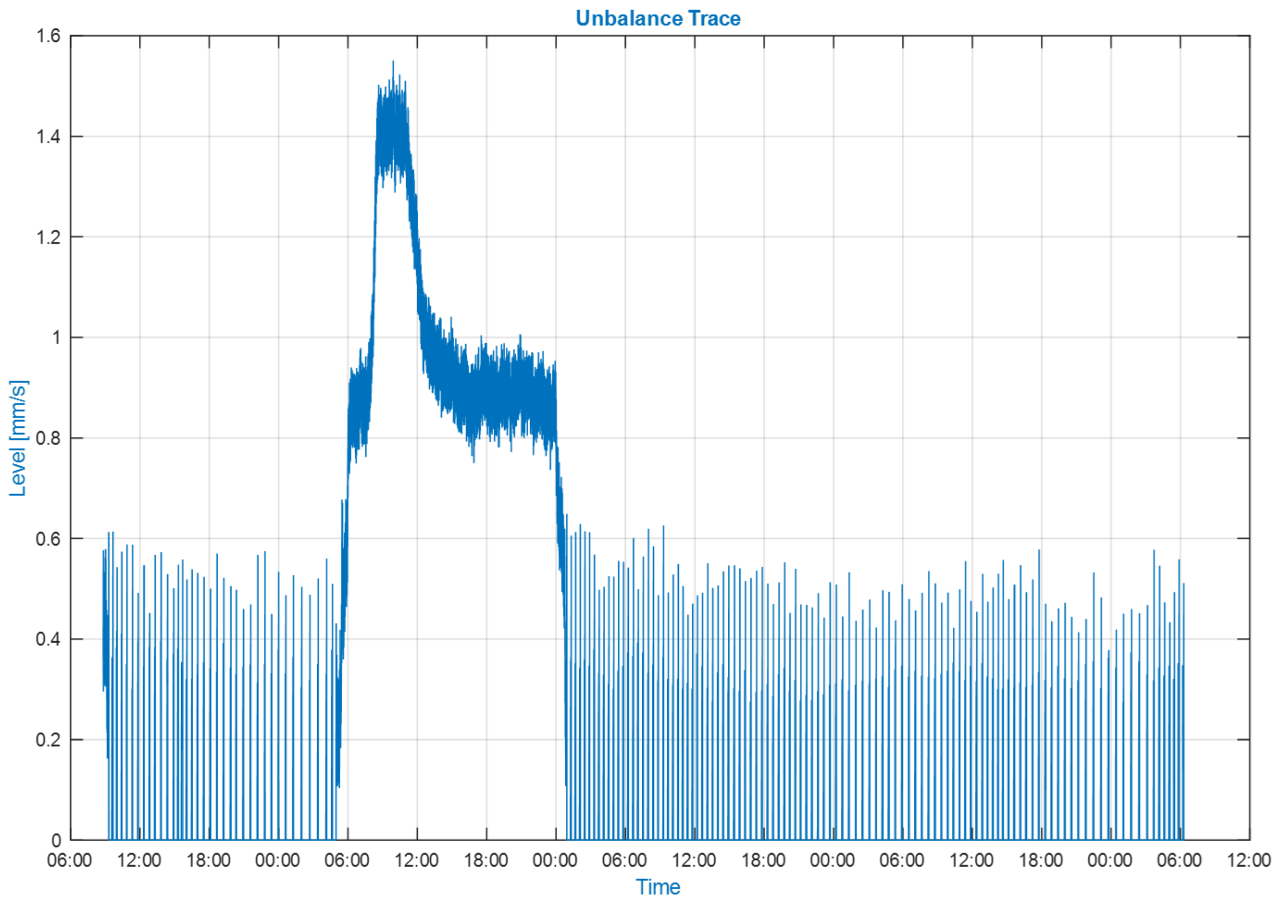

Figure 17: Plot of measured values for pump unbalance over a four-day period, with monitored data in a 1 sec. resolution.

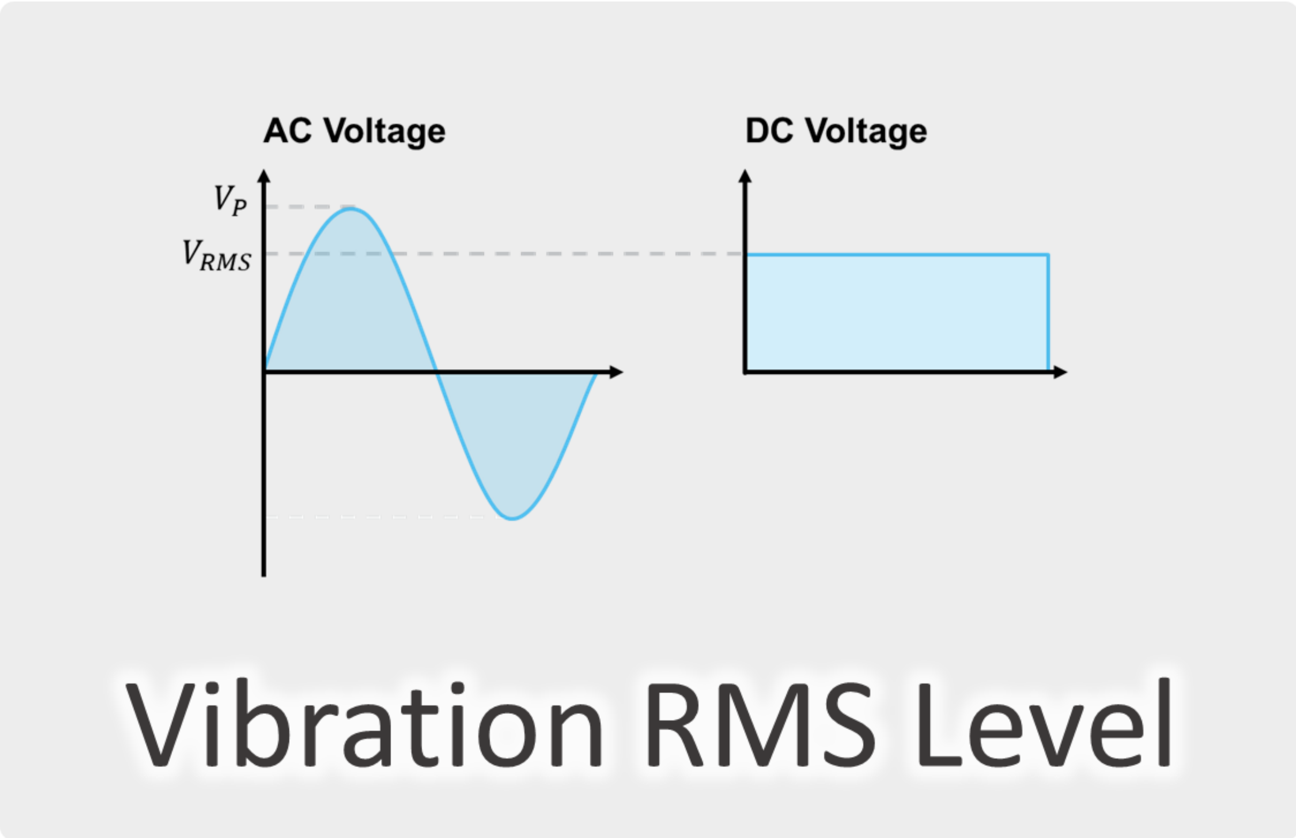

11. Vibration RMS

The classic measure of vibration level is the corresponding **R**oot **M**ean **S**quare (RMS) value, as this is the "effective value" of a signal with a dynamic nature.

One can say that it is the most popular numeric value describing average "**vibration level"** of a certain machine. On the other hand, it does not provide much insight into the source of the vibration.

The *Root* element indicates calculating (in the last step) a square root, the second element *Mean* indicates mean value and the third Square indicates that each value of the signal is squared, see Figure 18.

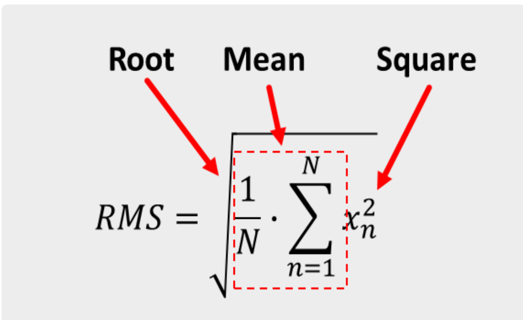

Figure 18: Calculation of the Vibration RMS.

The sequence of operation is inverted relative to consecutive letters in the RMS abbreviation.

An RMS value is also known as the effective value and is defined in terms of the equivalent heating effect of direct current. The RMS value of a sinusoidal voltage (or any time-varying voltage) is equivalent to the value of a dc voltage that causes an equal amount of heat - as illustrated in the chapter figure above. For a sinewave with amplitude A, the corresponding RMS level is simply A/1.41.

The ISO standard ISO-20816 states that the vibration signal must be measured "in a broad frequency range reaching from at least 10Hz to 1.000Hz".

The ANSI standard states that "The unfiltered root-mean-squared (RMS) vibration reading shall be recorded at the top motor bearing location".

To be able to compare measurements with severity charts, it is important to align specifications regarding filtering, sensor position etc. Examples of characteristics are stated in the following Figure 19.

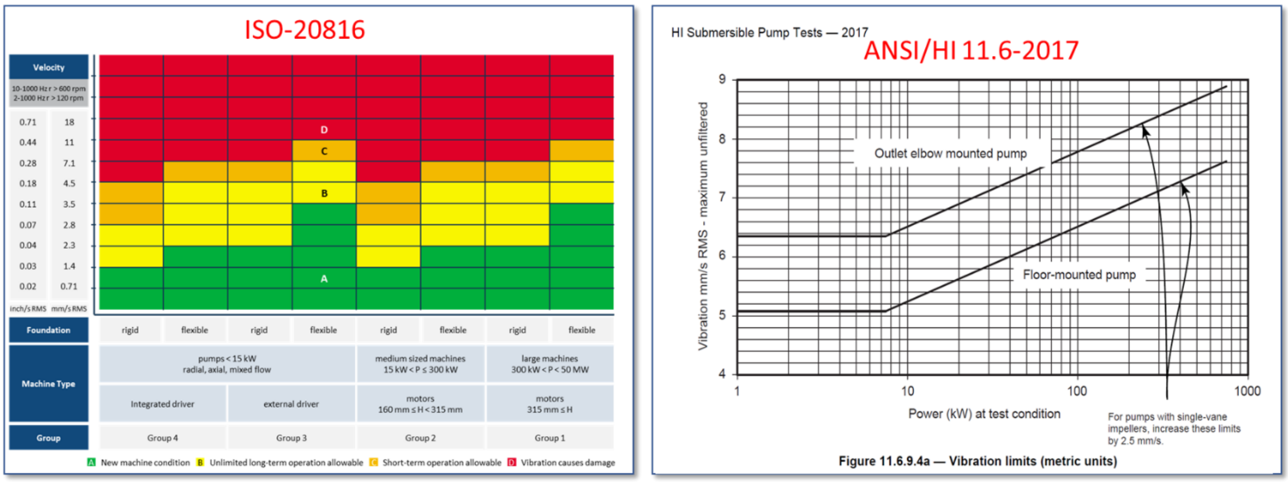

Figure 19: Left picture is from the ISO-20816 standard. Right plot is from ANSI/HI 11.6-2017 standard.

It should be noted, from using Parseval's Theorem, that the RMS value can both be calculated from the vibration time waveform and from the corresponding Vibration spectra.

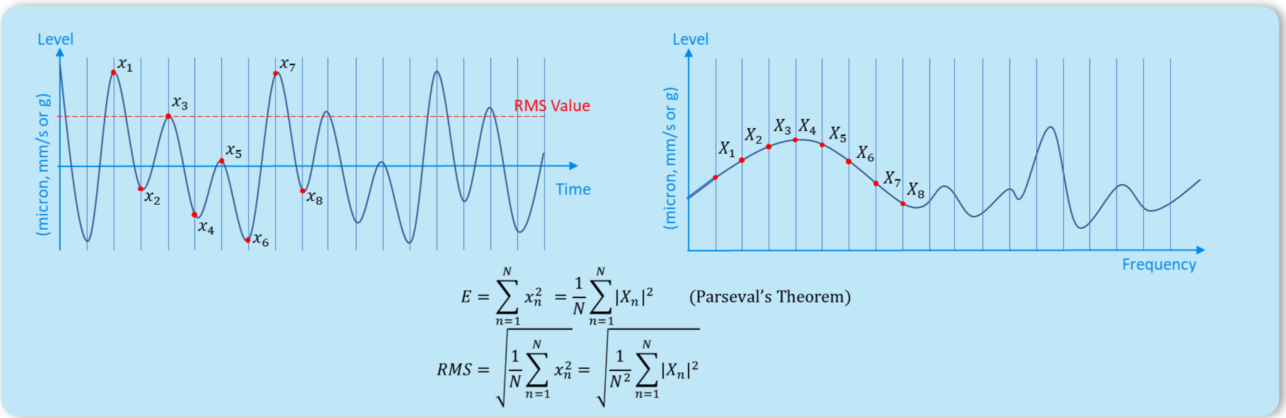

Figure 20: How the EWA sensor are calculating the Vibration RMS value.

The EWA sensor algorithm for Vibration RMS calculates the value as RMS value of the bandpass filtered (10-1.000Hz) velocity spectra with four averages, following the recommendation from ISO-20816.

Another signal metric closely related to the RMS is the Crest Factor or Peak Factor. The Crest factor is a dimensionless ratio used to characterize a waveform. The term defines the ratio between the Peak values (either positive or negative) of a waveform to its RMS value, and is a measure of how far the waveform deviates from its average value:

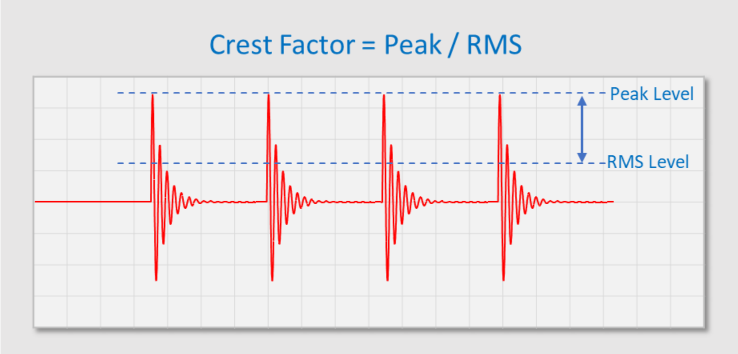

Figure 22: Illustration of the Crest Factor, relating peak and RMS levels into one performance parameter.

When the Crest Factor increases, it indicates that the waveform is becoming more peaked, and it is used in many applications to indicate a possible failure. As a peak detector, the Crest Factor is more sensitive than the RMS value, as indicated in the following case, involving a defect spring in a non-return valve in a pumping station:

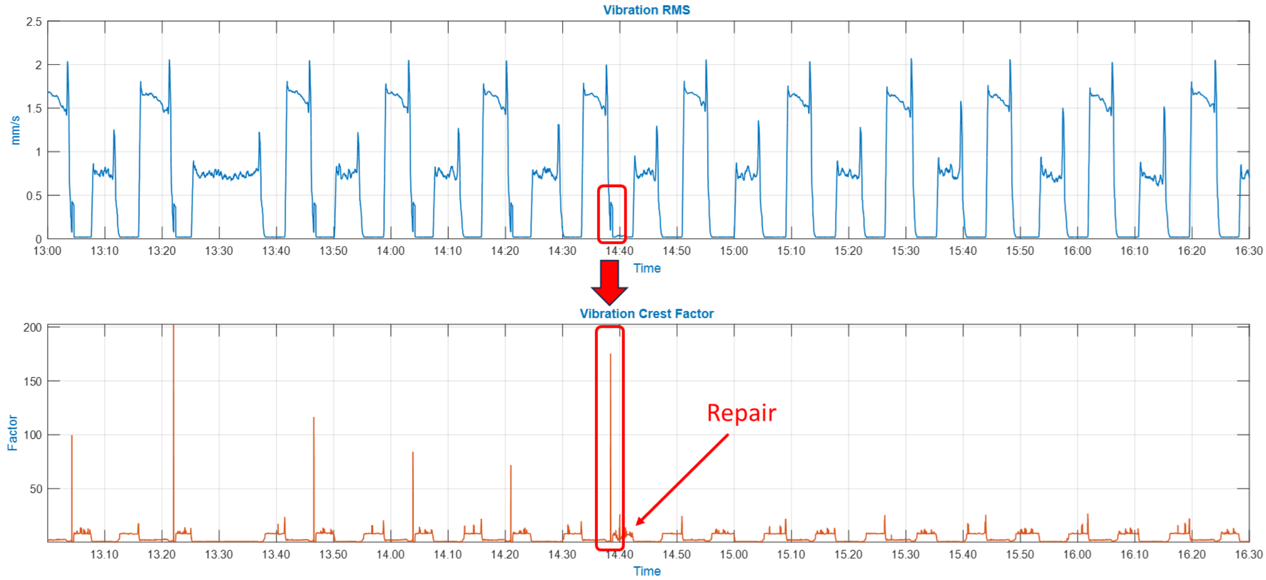

Figure 21: Illustration of corresponding measurement of Vibration RMS and Vibration Crest Factor, for an application with a non-return valve with a broken spring. The broken spring has been exchanged at 14:40.

The actual valve is a non-return valve from AVK[1]:

"The spring tension ensures fast and gentle closing which prevents water hammer. If a pump stops and the forward flow reverses back down the line towards the pump, before the check valve has fully closed, the flow will force the valve door to slam onto its seat. This scenario can almost instantaneously stop the reverse flow and it is this instantaneous stoppage which results in pipeline water hammer. This can produce loud hammer noises which is not the noise of the valve coming into its seated position but is the stretching of the pipe under these conditions."

[1] AVK UK, "An Introduction to Non-Return Valves and the Importance of Correct Selection".

Broken spring Operating spring

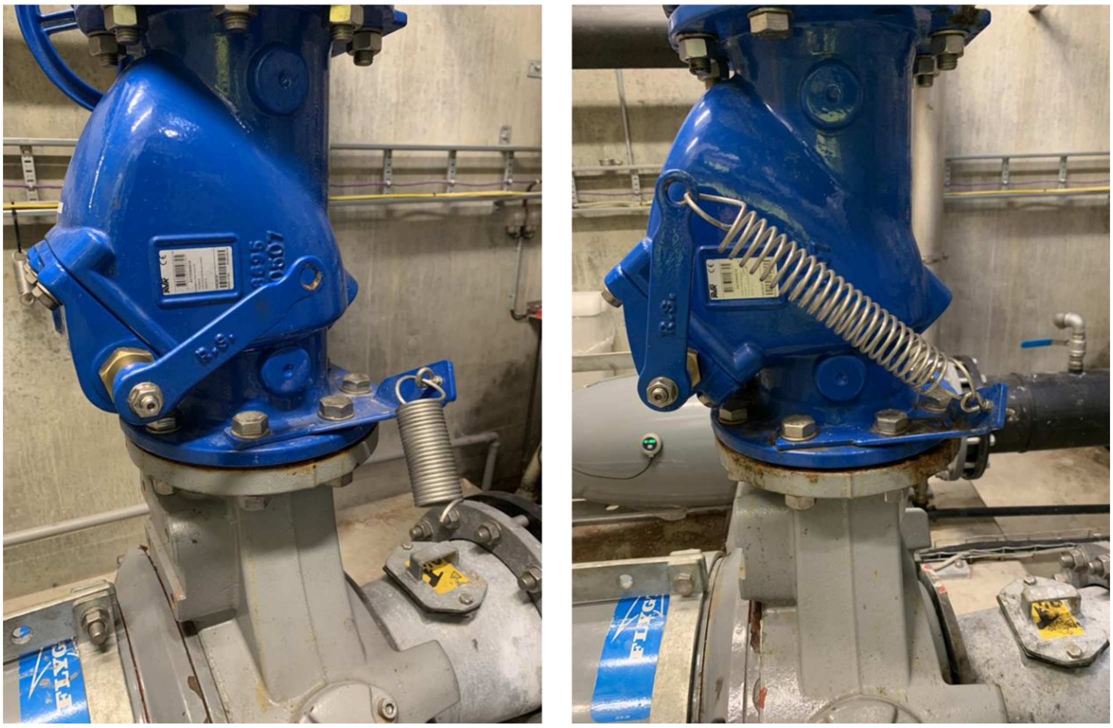

Figure 23: Pictures from an application. Picture to the left illustrates the broken non-return valve spring, and the picture to the right shows the valve with a new inserted spring.

Besides RMS and Crest Factor, the EWA sensor also calculates signal metrics like Sample Standard deviation, Kurtosis, and Skewness.

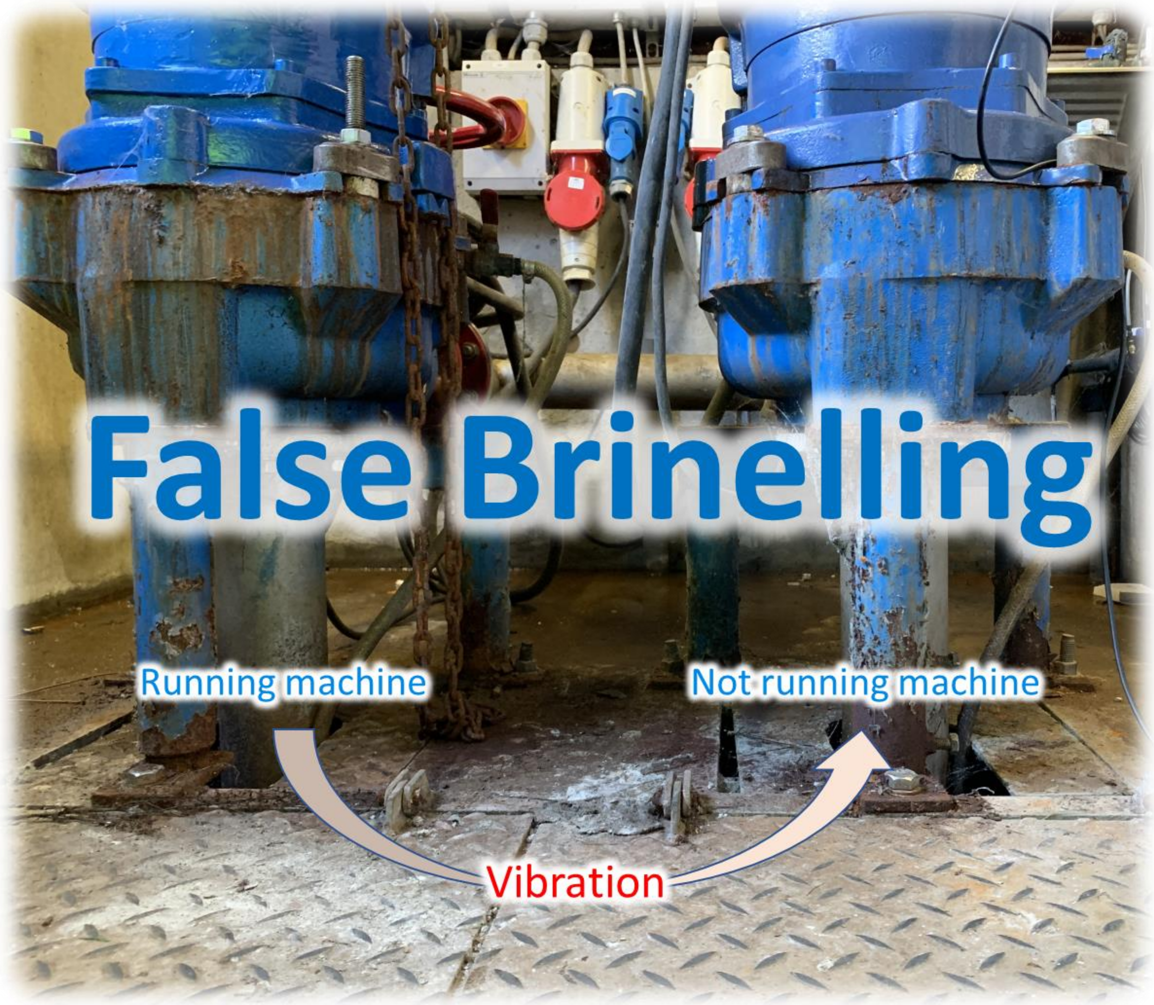

12. False Brinelling

Forcing a machinery to vibrate, while it is not operating, can be very harmful to machine parts like shaft seals and bearings. These vibration impacts can originate from transportation to customers, but they can also come from surrounding operating machinery after installed at customer site.

When the machine is installed, the vibration impacting a machine will come from two sources: primarily impact from self-induced vibration during operation, and secondary impact from surrounding machinery while the machine itself is not operating.

When talking of bearing and bearing damage, this type of damaging vibration has been named ”False Brinelling” in the literature. When a machine with ball bearing is in operation, the bearing balls are rotating in the race ways, and the loading from the shaft + vibration is distributed over the surface of the race ways. But when the machine bearing is not operating, the balls are in a fixed position, and all load + vibration will impact the bearing race area on a limited number of points (number of balls).

Figure 24: A damaged bearing, due to false brinelling.

The damage from false brinelling can visually be inspected by disassembling the bearing. It has a distinguished pattern - see Figure 24.

The EWA sensor measures the level of False Brinelling on a machine as a ratio between the received vibration energy while the machine is not operating ($E_{Stopped}$) compared to the total received vibration energy ($E_{Stopped}$+ $E_{Running}$):

$$False\ Brinelling = \frac{E_{Stopped}}{E_{Stopped} + E_{Running}} \cdot 100\%$$

The False Brinelling Ratio is calculated on a 24-hour basis. From the RPM parameters, the sensor knows when the motor is running and when it is stopped. The principle can be seen from the figure below.

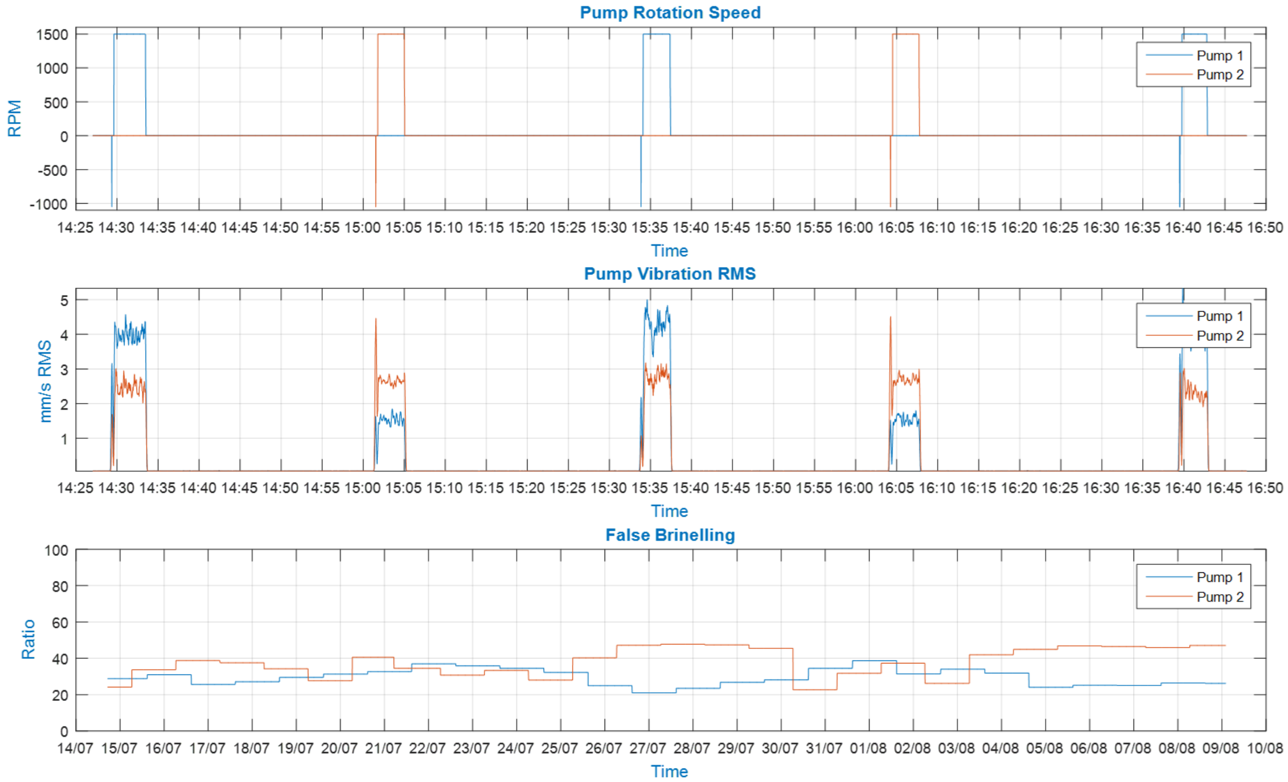

Figure 25: Upper plot illustrates the pump rotation speed. The middle plot illustrates the corresponding measured Vibration RMS. Bottom plot illustrates the calculated value for False Brinelling (False Brinelling ratio), plotted for a time-period of 28 days.

The top graph illustrates the measured RPM from an installation with two pumps. The pumps are operating in an alternating mode, where each pump starts with a short reverse rotation. The second graph illustrates the corresponding measured Vibration RMS level for the same time-period as shown in top graph. By inspecting the first operation cycle of pump 1, a considerable level of vibration is transferred to the non-running pump 2. The same observation can be seen during the first operation cycle of pump 2. For this installation, the False Brinelling ratio is up to 39% for pump 1 and 50% for pump 2.

Vibrations are often transferred between machines through stiff piping or coupled foundation.

General Bearing Fault Detection algorithm will first detect a bearing defect, when the bearing has become damaged, but the False Brinelling algorithm will detect an installation issue from *day one of operation*, and proper intervention can be initiated to prevent bearing damage. It is a measure of installation quality.

From a machine manufacture point of view, it is a strong tool for root-cause-analysis in warranty cases with premature bearing break down.

A last illustration of the False Brinelling problem is from a pumping station with two 37kW pumps installed.

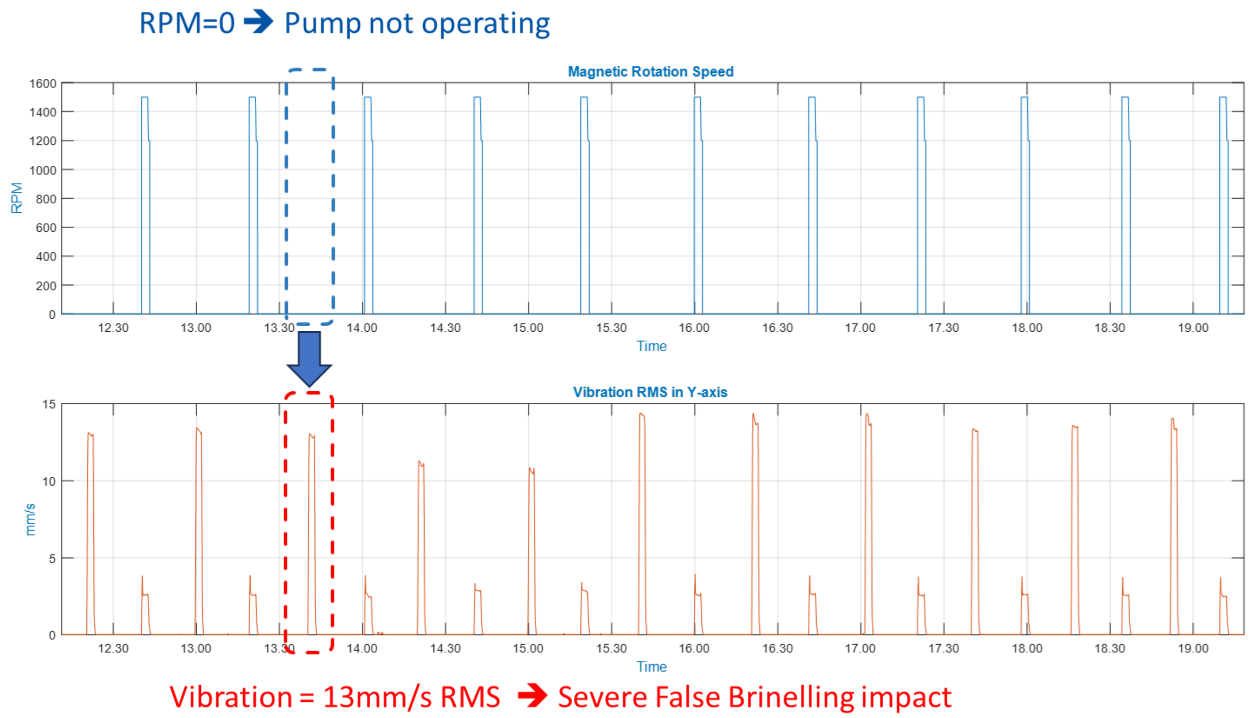

Figure 26: Monitoring data from a real application. Upper figure illustrates motor RPM and the lower plot illustrates the corresponding Vibration RMS level. A time interval has been highlighted where the machine is not operating, but it is vibrating considerable. From the Vibration RMS data, the vibration level is 2.6 mm/s while operating and 13 mm/s while not operating.

In this case, vibration from a second running pump provides a vibration contribution 5x larger, compared to when the pump is running itself.

The case in Figure 26 corresponds to a False Brinelling factor of 82% for a 24-hour period. The root cause could be a soft foundation, combined with gyro stabilization during normal operation.

The False Brinelling algorithm has an EWA patent.

13. Cavitation

One of the classical issues with pump systems is Cavitation. It is a formation of vapor bubbles within a liquid at low-pressure regions in the machine, that occurs in places where the liquid has been accelerated to high velocities, as seen in the operation of centrifugal pumps, water turbines, and marine propellers.

Cavitation is undesirable because it produces extensive erosion of the rotating blades, additional noise from the resultant knocking and vibrations, and a significant reduction of efficiency, because it distorts the flow pattern and creates fluctuations of pump speed. It's a symptom of insufficient net positive suction head.

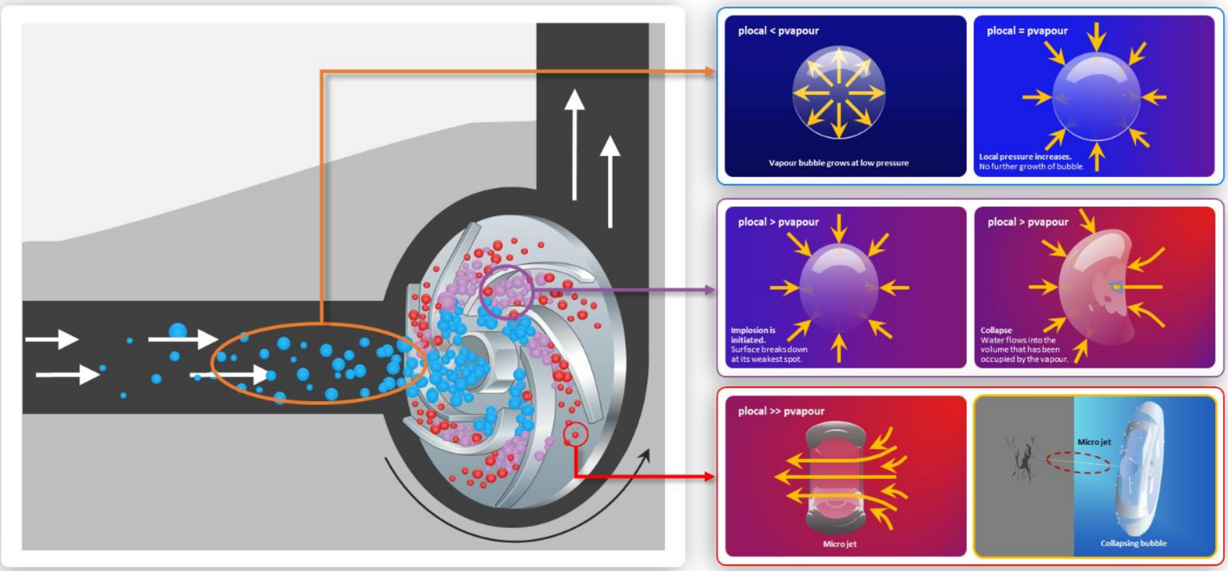

Figure 27: Illustration of vapor bubbles in a pump system, showing the development of cavitation in the pump impeller.

To some extent, a small level of harmless cavitation is always present in pump system. When cavitation is measurable using vibration analysis, it is a sign of erosion of the rotating blades, and service intervention are needed.

Some of the known tell-tale signs of pump cavitation are:

- Random bursts of energy – separated with 1-3 seconds.
- Vibration level for axial direction > radial direction (lower axial stiffness).
- Sounds like “marbles” or “gravel” are passing through the pump.
- Unstable flow and fluctuations of pump speed.

The EWA sensor Cavitation algorithm is based on a perceptual approach, to capture the modulation level of the random bursts of high frequency energy, that can be heard standing next to a cavitating pump. It is not the high frequency vibration energy, but the random bursts of high frequency energy that signal cavitation.

The level of cavitation is estimated as a path length over 10 seconds – illustrated as a blue curve in the following figure for both a cavitation case, and a non-cavitation case.

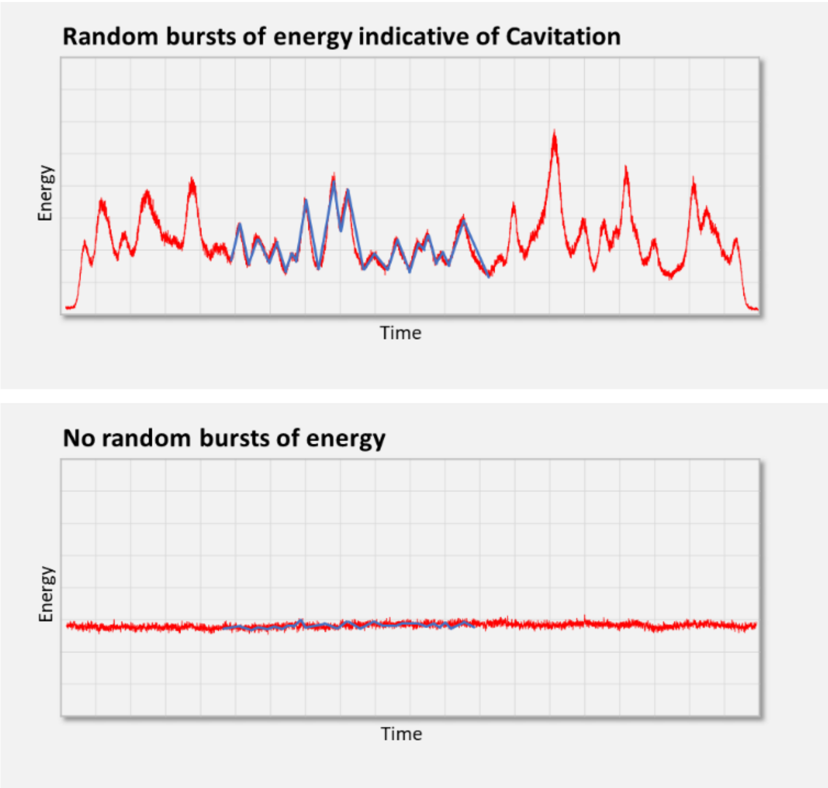

Figure 28: Top figure shows the energy content when cavitation occurs. The bottom curve illustrates the energy content when no cavitation is present.

An initial baseline level of this path length is established during the baseline initialization period, and used for normalization of both the cavitation parameter, baseline and baseline initialization level, and values are transmitted on the Modbus.

To illustrate the path length approach for a real-life application, measurement on a 30kW wastewater pump is used. Below, normal pump operation for 5-minute is followed with a 30-minute cavitation period (inlet pressure reduced), and again followed with a 5-minute of normal operation period without any cavitation, see Figure 29.

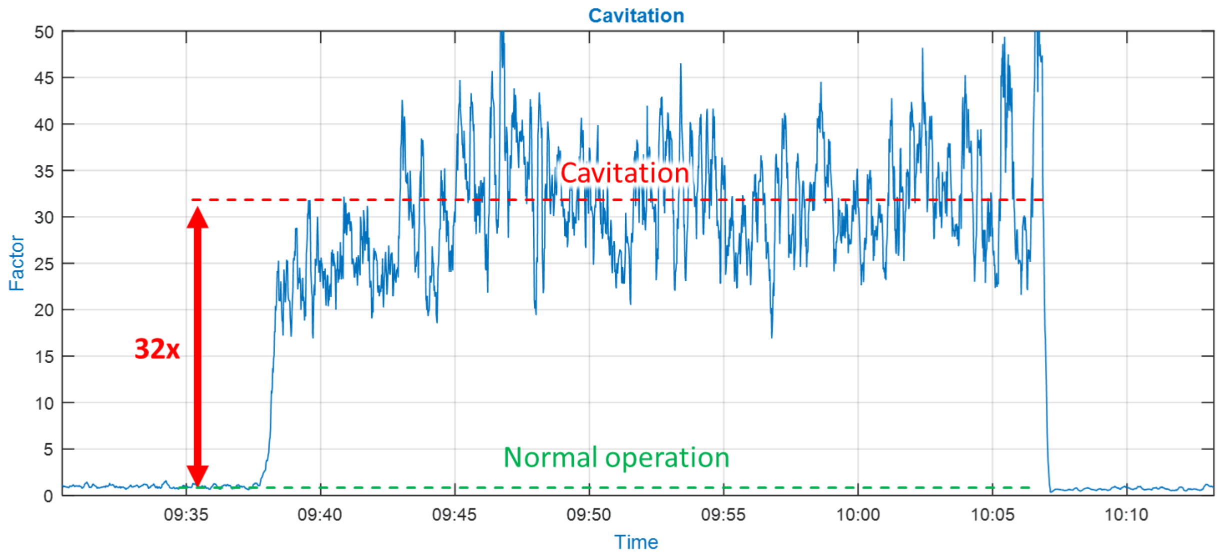

Figure 29: Cavitation occurs at 9:38 and is present until 10:07.

The feature gain factor, defined as the difference between normal mean value and cavitation mean value, is 32x for this *path approach* for cavitation detection, see Figure 29.

To compare the outcome of the Cavitation algorithm to other parameters like the Vibration RMS and Unbalance, the Vibration RMS and Unbalance parameter data monitored during a cavitation period are plotted in the following two graphs, in Figure 30. The feature gain factor for Vibration RMS and Unbalance is respectively 1.24 and 1.25.

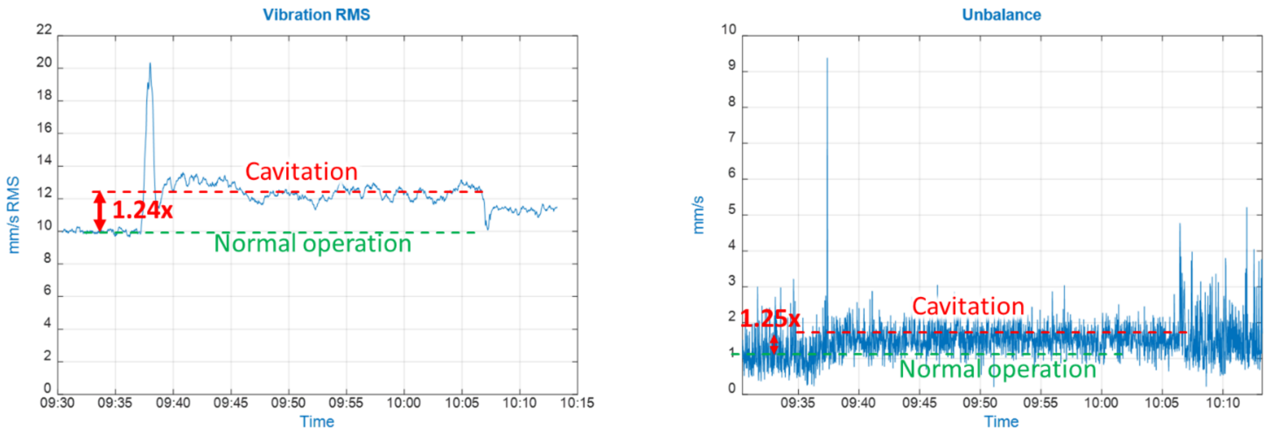

Figure 30: Monitored parameters for Vibration RMS and Unbalance, on the time when cavitation occurs.

14. Bearing Fault detection

Bearings are key machine components in any rotation machinery, and under normal operation they just produce a low level of vibration of a random nature. When a fault is developing inside the bearing, the bearing's vibration pattern changes and the overall vibration level increases.

In the case of an initial point damage (like a crack), the vibration pattern shifts from a low-level random nature to a higher level of periodic nature. Every time a ball role over a crack, a high vibration sound is produced, and the impact frequency of the crack is proportional to the shaft RPM.

Four different impact frequencies are produced dependent on the location of the crack – on the outer race (Ball Pass Frequency Outer race, BPFO), inner race (Ball Pass Frequency Inner race, BPFI), balls (Ball Spin Frequency, BSF) or cage (Fundamental Train Frequency, FTF) – also known as the Characteristic Defect Frequencies (CDF). Under normal working condition, a bearing should not produce its CDF, so the present of one of these frequencies in the vibration signal is a strong indicator of a bearing issue.

The CDF are property of the bearing geometry, rotational speed, and number of rolling elements and are easily calculated frequencies (noted Ω), as shown in the calculations in Figure 31 below.

The Four Characteristic Bearing Frequencies

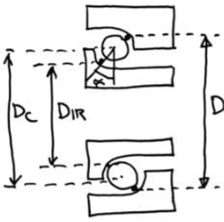

D_C = Cage diameter
D_{IR} = Inner raceway dia
D_{OR} = Outer raceway di
D_B = Ball diameter
α = Contact angle
N_B = Number of Ball

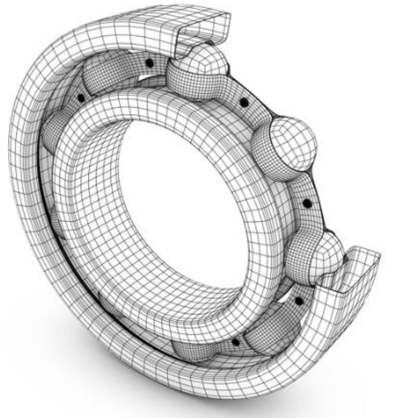

Point velocity on a circle : $V = f \cdot O = f \cdot r \cdot 2 \cdot \pi$

Diameter of inner and outer raceway:

$$D_{IR} = D_C - 2 \cdot \left(\frac{D_B}{2} \cdot \cos(\alpha)\right) = D_C - D_B \cdot \cos(\alpha)$$

$$D_{OR} = D_C + 2 \cdot \left(\frac{D_B}{2} \cdot \cos(\alpha)\right) = D_C + D_B \cdot \cos(\alpha$$

1. Fundamental Train Frequency, FTF

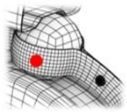

$$V_{IR} = \Omega_{IR} \cdot \frac{D_{IR}}{2} = \frac{\Omega_{IR}}{2} \cdot \left(D_C - D_B \cdot \cos(\alpha)\right)$$

$$V_{OR} = \Omega_{OR} \cdot \frac{D_{OR}}{2} = \frac{\Omega_{OR}}{2} \cdot \left(D_C + D_B \cdot \cos(\alpha)\right)$$

$$V_C = \frac{V_{IR} + V_{OR}}{2} = \frac{1}{2}\left(\frac{\Omega_{IR}}{2}\left(D_C - D_B \cdot \cos(\alpha)\right) + \frac{\Omega_{OR}}{2}\left(D_C + D_B \cdot \cos(\alpha)\right)\right)$$

$$\Omega_C = \frac{V_C}{0{,}5 \cdot D_C} = \left(\frac{\Omega_{IR}}{2}\left(1 - \frac{D_B}{D_C} \cdot \cos(\alpha)\right) + \frac{\Omega_{OR}}{2} \cdot \left(1 + \frac{D_B}{D_C} \cdot \cos(\alpha)\right)\right)$$

$$= \frac{1}{2} \cdot \left(\Omega_{IR} \cdot \left(1 - \frac{D_B}{D_C} \cdot \cos(\alpha)\right) + \Omega_{OR} \cdot \left(1 + \frac{D_B}{D_C} \cos(\alpha)\right)\right)$$

$$V_{OR} = 0 \quad \Rightarrow \quad \boxed{\Omega_C = \frac{\Omega_{IR}}{2} \cdot \left(1 - \frac{D_B}{D_C} \cdot \cos(\alpha)\right)}$$

2. Ball Pass Frequency Inner race, BPFI

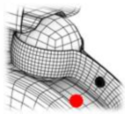

$$\Omega_I = N_B \cdot \left|\Omega_C - \Omega_{IR}\right|$$

$$= N_B \cdot \left|\frac{1}{2} \cdot \left(\Omega_{IR}\left(1 - \frac{D_B}{D_C} \cdot \cos(\alpha)\right) + \Omega_{OR}\left(1 + \frac{D_B}{D_C} \cdot \cos(\alpha)\right)\right) - \Omega_{IR}\right|$$

$$= N_B \cdot \left|\frac{\Omega_{IR}\left(D_C - D_B \cdot \cos(\alpha)\right) + \Omega_{OR}\left(D_C + D_B \cdot \cos(\alpha)\right) - 2 D_C \cdot \Omega_{IR}}{2 \cdot D_C}\right|$$

$$= N_B \cdot \left|\frac{\Omega_{IR} \cdot D_C - \Omega_{IR} D_B \cdot \cos(\alpha) + \Omega_{OR} D_C + \Omega_{OR} D_B \cos(\alpha) - 2 D_C \Omega_{IR}}{2 \cdot D_C}\right|$$

$$= N_B \cdot \left|\frac{-\Omega_{IR} \cdot D_C + \Omega_{OR} D_C - \Omega_{IR} D_B \cdot \cos(\alpha) + \Omega_{OR} \cdot D_B \cdot \cos(\alpha)}{2 D_C}\right|$$

$$= N_B \cdot \left|\frac{\left(\Omega_{OR} - \Omega_{IR}\right) \cdot \left(D_C + D_B \cdot \cos(\alpha)\right)}{2 \cdot D_C}\right|$$

$$= N_B \cdot \left|\left(\Omega_{OR} - \Omega_{IR}\right)\left(\frac{1}{2} + \frac{D_B \cdot \cos(\alpha)}{2 \cdot D_C}\right)\right|$$

$$\Omega_{OR} = 0 \quad \Rightarrow \quad \boxed{\Omega_I = \frac{N_B \cdot \Omega_{IR}}{2} \cdot \left(1 + \frac{D_B}{D_C} \cdot \cos(\alpha)\right)}$$

3. Ball Pass Frequency Outer race, BPFO

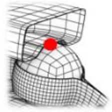

$$\Omega_O = N_B \cdot \left|\Omega_C - \Omega_{OR}\right|$$

$$= N_B \cdot \left|\frac{1}{2} \cdot \left(\Omega_{IR} \cdot \left(1 - \frac{D_B}{D_C} \cdot \cos(\alpha)\right) + \Omega_{OR} \cdot \left(1 + \frac{D_B}{D_C} \cdot \cos(\alpha)\right)\right) - \Omega_{OR}\right|$$

$$= N_B \cdot \left|\frac{\Omega_{IR}\left(D_C - D_B \cos(\alpha)\right) + \Omega_{OR}\left(D_C + D_B \cdot \cos(\alpha)\right) - 2 \cdot D_C \cdot \Omega_{OR}}{2 \cdot D_C}\right|$$

$$= N_B \cdot \left|\frac{\Omega_{IR} \cdot D_C - \Omega_{IR} D_B \cdot \cos(\alpha) + \Omega_{OR} \cdot D_C + \Omega_{OR} \cdot D_B \cdot \cos(\alpha) - 2 D_C \cdot \Omega_{OR}}{2 \cdot D_C}\right|$$

$$= N_B \cdot \left|\frac{\Omega_{IR} \cdot D_C - \Omega_{OR} \cdot D_C - \Omega_{IR} D_B \cos(\alpha) + \Omega_{OR} \cdot D_B \cdot \cos(\alpha)}{2 \cdot D_C}\right|$$

$$= N_B \cdot \left|\frac{\left(\Omega_{IR} - \Omega_{OR}\right) \cdot \left(D_C - D_B \cdot \cos(\alpha)\right)}{2 \cdot D_C}\right|$$

$$= N_B \cdot \left|\left(\Omega_{IR} - \Omega_{OR}\right) \cdot \left(\frac{1}{2} - \frac{D_B \cdot \cos(\alpha)}{2 D_C}\right)\right|$$

$$\Omega_{OR} = 0 \quad \Rightarrow \quad \boxed{\Omega_O = \frac{N_B \cdot \Omega_{IR}}{2} \cdot \left(1 - \frac{D_B}{D_C} \cdot \cos(\alpha)\right)}$$

4. Ball Spin Frequency, BSF

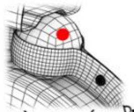

$$\Omega_B = \left(\Omega_{IR} - \Omega_C\right) \frac{D_{IR}}{D_B}$$

$$= \left(\Omega_{IR} - \frac{1}{2} \Omega_{IR}\left(1 - \frac{D_B}{D_C} \cdot \cos(\alpha)\right) + \Omega_{OR} \cdot \left(1 + \frac{D_B}{D_C} \cos(\alpha)\right)\right) \cdot \frac{D_C - D_B \cdot \cos(\alpha)}{D_B}$$

$$= \left(\Omega_{IR} - \frac{1}{2 D_C} \cdot \Omega_{IR}\left(D_C - D_B \cdot \cos(\alpha)\right) + \Omega_{OR} \cdot \left(D_C + D_B \cdot \cos(\alpha)\right)\right) \cdot \frac{D_C - D_B \cdot \cos(\alpha)}{D_B}$$

$$= \left(\Omega_{IR} - \frac{\Omega_{IR}}{2 D_C} \cdot \left(D_C - D_B \cdot \cos(\alpha)\right) + \frac{\Omega_{OR}}{2 D_C} \cdot \left(D_C + D_B \cdot \cos(\alpha)\right)\right) \cdot \frac{D_C - D_B \cdot \cos(\alpha)}{D_B}$$

$$= \frac{\Omega_{IR}}{D_B} \cdot \left(D_C - D_B \cdot \cos(\alpha)\right) - \frac{\Omega_{IR}}{2 D_C D_B} \cdot \left(D_C - D_B \cdot \cos(\alpha)\right)^2$$

$$- \frac{\Omega_{OR}}{2 D_C D_B} \cdot \left(D_C + D_B \cdot \cos(\alpha)\right) \cdot \left(D_C - D_B \cdot \cos(\alpha)\right)$$

$$= \Omega_{IR} \cdot \frac{D_C}{D_B} - \Omega_{IR} \cdot \cos(\alpha) - \frac{\Omega_{IR}}{2 D_C D_B} \cdot \left(D_C^2 - 2 D_C D_B \cdot \cos(\alpha) + D_B^2 \cdot \cos^2(\alpha)\right)$$

$$- \frac{\Omega_{OR}}{2 \cdot D_C \cdot D_B} \cdot \left(D_C^2 - D_C D_B \cdot \cos(\alpha) + D_C D_B \cdot \cos(\alpha) - D_B^2 \cdot \cos^2(\alpha)\right)$$

$$= \Omega_{IR} \cdot \frac{D_C}{D_B} - \frac{\Omega_{IR} \cdot D_C}{2 D_B} - \frac{\Omega_{IR} \cdot D_B}{2 D_C} \cdot \cos^2(\alpha) - \frac{\Omega_{OR} \cdot D_C}{2 \cdot D_B} + \frac{\Omega_{OR} D_B}{2 D_C} \cdot \cos^2(\alpha)$$

$$= \left(\Omega_{IR} - \Omega_{OR}\right) \cdot \frac{D_C}{2 D_B} - \left(\Omega_{IR} - \Omega_{OR}\right) \frac{D_B}{2 D_C} \cdot \cos^2(\alpha)$$

$$= \frac{D_C}{2 D_B} \cdot \left(\Omega_{IR} - \Omega_{OR}\right) \cdot \left(1 - \frac{D_B^2}{D_C^2} \cdot \cos^2(\alpha)\right)$$

$$\Omega_{OR} = 0 \quad \Rightarrow \quad \boxed{\Omega_B = \frac{D_C \cdot \Omega_{IR}}{2 \cdot D_B} \cdot \left(1 - \frac{D_B^2}{D_C^2} \cdot \cos^2(\alpha)\right)}$$

Figure 31: Calculations for the four fundamental Characteristic Defect Frequencies (CDF).

To make the CDF independent of the shaft RPM, bearing manufactures often normalize the four fundamental frequencies with the shaft rotation speed (Xfactor=CDF/RPM) in the datasheet. When a given Xfactor has been determined from a vibration recording, the corresponding fault can be identified from bearing manufactures data sheet. A bearing like the SKF6308 bearing has the following Xfactor valuess: FTF=0.384, BPFI=4.92, BPFO=3.07 and BSF=4.08, all independent of the shaft rotation speed.

In practical cases, a fault on a ball will often hit both inner and outer race during rotation, and thereby produces a 2*BSF frequency.

However, a challenge using the CDF approach for bearing fault detection in real life is, that the actual bearing data in an installation often is unknown. The nameplate might state DE=6308 (bearing number for Drive End), but it only guarantees the external geometry for the installation, but CDF is related to the internal geometry of the bearing. Manufactures may use different numbers of balls for the same bearing number, and thereby having different CDF values for the same bearing number.

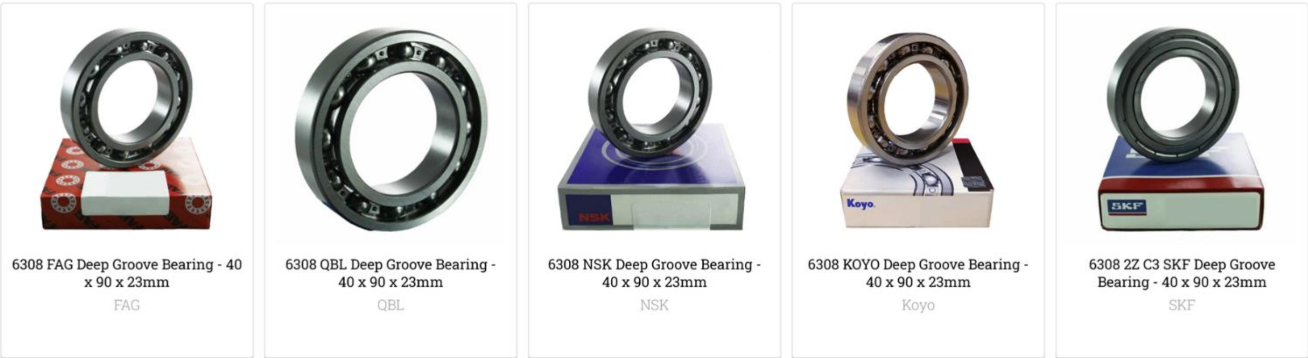

Figure 32: A bearing like the 6308 is offered by all major bearing companies.

Pump and motor manufactures often do not have traceability on bearing brands used in the machine production, but only the bearing number, and after the first service overhauling, nobody knows which brand of bearings being installed in the machine.

It should be noted that one very important property of bearing's Xfactors are, that they are not integer multiples of shaft rotational speed. This characteristic allows us to suspect a potential bearing problem, even if the bearing type is unknown. If the vibration data contains a non-synchronous vibration above the RPM (like 3.18X), or sub-synchronous vibration below the RPM (like 0.4X), it is highly likely related to the bearings, as no other machine component will produce that signature. It will tell us about a bearing issue, but it will not tell us whether the bearing problem is within the inner or outer race of the DE or NDE bearing (but this is often of no concern – the bearing will be identified during overhauling/service and replaced).

Every time a ball role over a crack, it will ping the impulse response of the mechanical resonance structure of the bearing. This means, that the vibration signal will contain a periodic part (time-period T) related to this crack, and the energy (E) of the impulse response will be related to the size of the crack, and thereby the severity of the fault. The impact frequency is the number of impact per second (1/T) – and this is given by the CDF.

- Impact frequency = 1/T = defect bearing part (inner/outer/ball/case)
- Impact energy = A = defect severity

A periodic signal will produce a line-spectrum, where the distance between the harmonics will be the impact frequency:

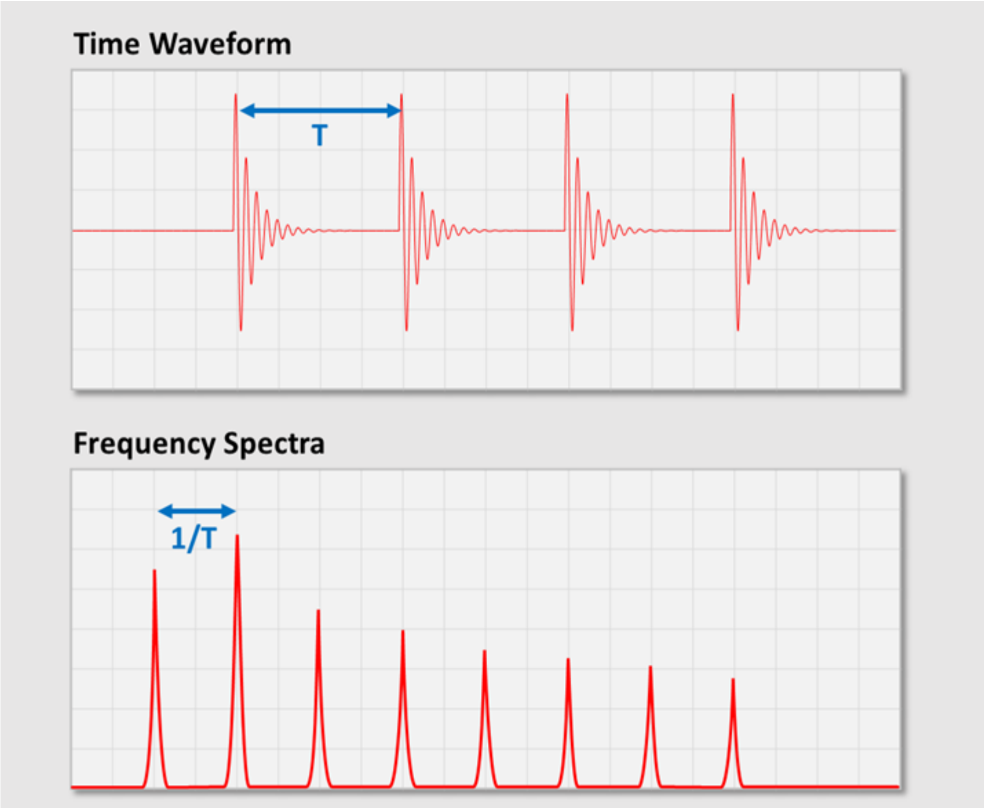

Figure 33: Illustration of the time period T in the Time Waveform, and the impact frequency 1/T in the Frequency Spectra.

The frequency content of the impulse response (bearing transfer function) does not contain information in relation to the actual bearing fault. Its content might start in the ultrasonic range and move down in frequency as the bearing fault start to evolve. The information in relation to bearing fault severity is contained in the impact frequency and its energy content.

From a signal analytic point of view, the vibration signal from a bearing crack is generated by a convolution between the impulse response function h(t) of the bearing and a pulse-train function d(t) from the crack. The information we seek is in the pulse-train function, and not in the impulse response function, so we need to separate the two functions again – to do a deconvolution of the vibration signal. A classical approach for deconvolution is the Cepstral transformation. It will separate the impulse response and the pulse-train into two non-overlapping regions, and thereby make it easy to inspect the pulse-train function.

The Cepstral transformation is simply a Power Spectrum of a logarithm Power Spectrum, and the procedure is illustrated in the following Figure 34.

In general, CDF should not be presented in a vibration signal, and the bearing severity measure will be zero. If the Bearing Fault Detection algorithm starts to detect an issue, the corresponding baseline must be observed to see how the fault develop. But when a non-zero severity measure is detected, it indicates a bearing issue and a coming bearing breakdown.

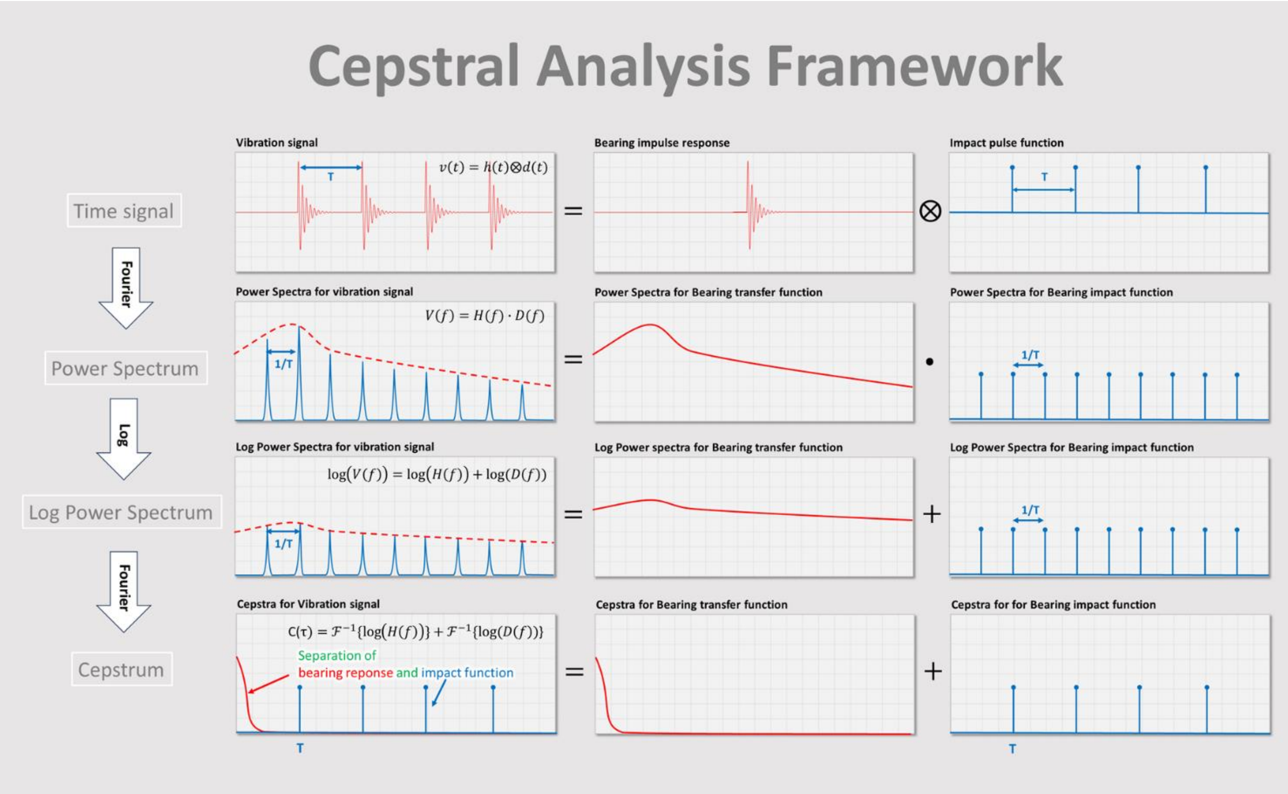

Figure 34: Illustration of an impulse signal in time domain, and the responding signals in power spectrum, log power spectrum and in Cepstrum.

The EWA sensor's *Bearing Fault Detection* algorithm analyzes the vibration signal for dominant non/sub synchronous contributions using Cepstral Analysis. When the same impact frequency is found in 10 consecutive measurements, the corresponding energy level and Xfactor are logged as a severity measure for the Bearing Fault Detection. The principle is illustrated in Figure 35 below.

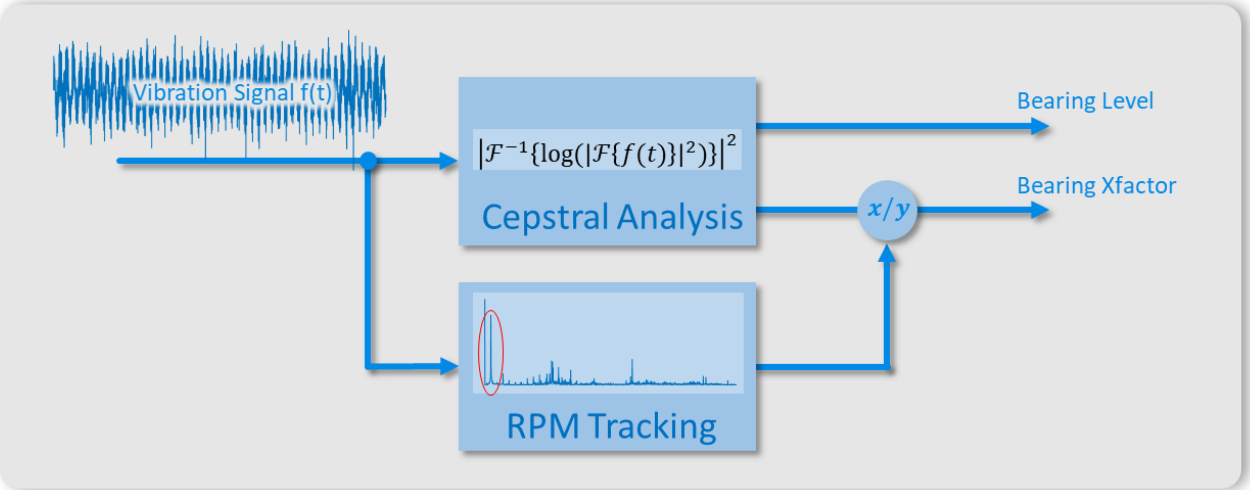

Figure 35: The actual bearing vibration level is found from a Cepstral analysis of the vibration signal.

As the level of the bearing fault energy depends on a range of factors (size of machine, distance between sensor and bearings etc.), the corresponding bearing Modbus parameters (level, baseline and initial baseline) will be normalized with the initial measured baseline level. The parameter will thereby express the development of the severity over time, relative to this machine. Levels and Xfactors are maintained for 60 minutes after last detection (end of operation).

The following case illustrates a detected bearing fault issue for a motor with 6308 and 3311 bearings.

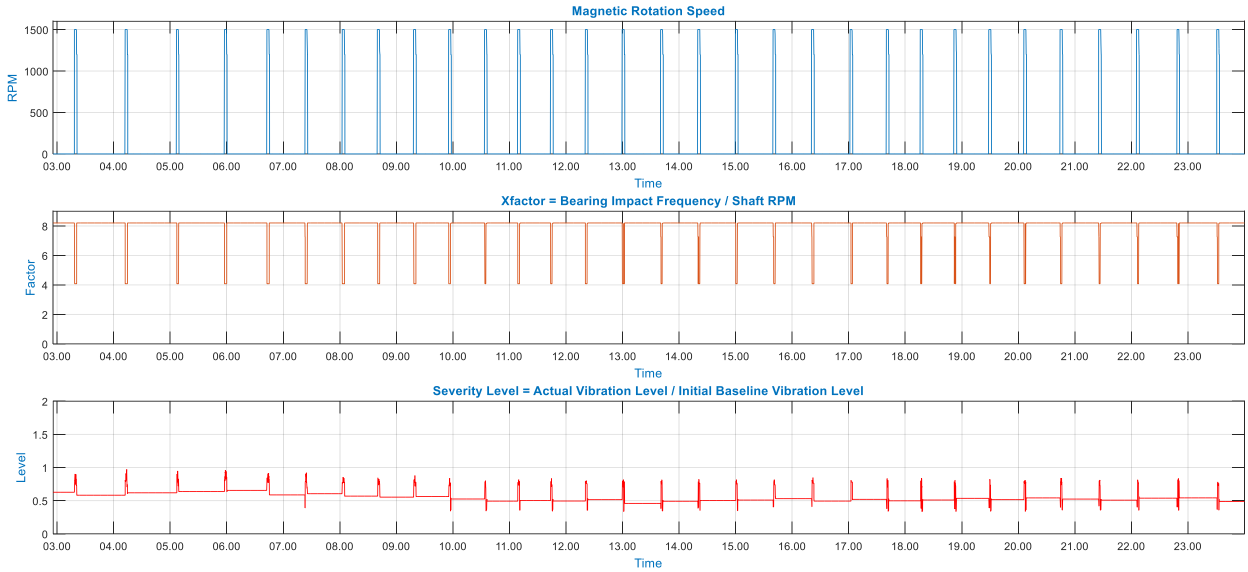

Figure 36: Bearing fault parameters for a case with a defect ball in a SKF6308 bearing.

The Xfactor measured in Figure 36 shows an alternation factor between 4.08 and 8.20 for this installation (Inspecting the datasheet for the SKF6308 state the BSF=4.078). Faults on bearing balls are known to produce double impact frequencies, as a point of damage hits both inner and outer race during one rotation (therefore the monitored Xfactor of 8.20). The core existence of a non-zero Xfactor is a very strong indicator of a bearing issue, but it might not be a problem. Many old installations will show sign of bearing wear but can run for many years. But if the severity level is doubled within weeks and cross the warning level, proactive action should be taking to replace the bearings.

15. Machine Looseness

The motion of a loose machine mounting bolt in its hole will not be exhibiting a smooth sinusoidal motion of rocking back and forth, but the signal will be truncated by the sides of the hold, and the corresponding motion will be something like a squared or chopped sinusoidal. The frequency spectrum will have many harmonics of the rotation frequency of the shaft (1X).

Mechanical looseness comes in many forms like structural frame looseness, cracked structure pedestal or improper fit between machine components, all signatured by an increasing number of harmonics in the vibration spectrum. Examples of looseness signatures are illustrated in the Figure 37.

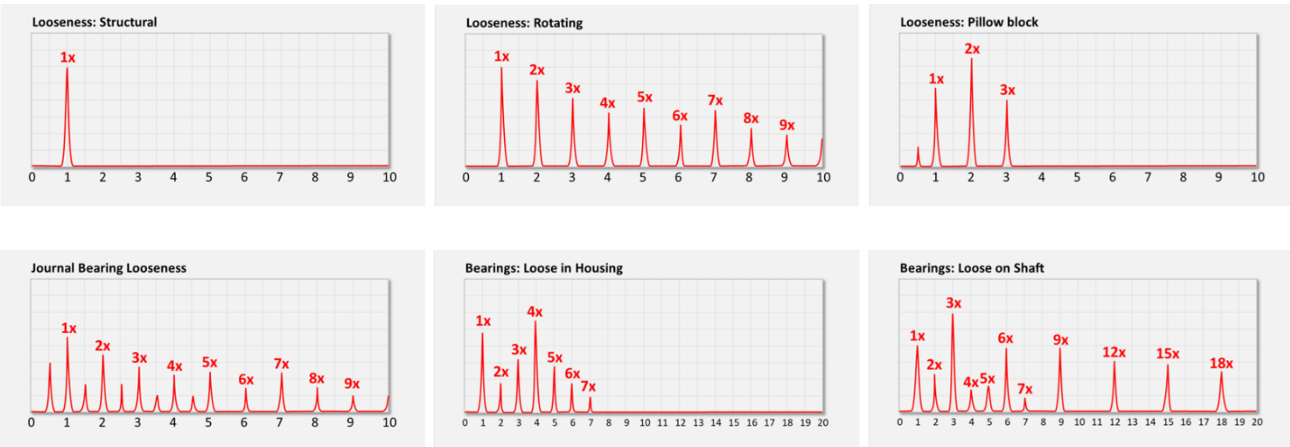

Figure 37: Signatures for different kind of machine looseness.

An important fact regarding each type of mechanical looseness is, that alone it is not a cause of vibration. Looseness is a reaction of other problems, like unbalance, misalignment, eccentricity, bearing problems etc.

Removing each of these problems will often remove the symptoms of looseness, but the issue remains. Looseness aggravates the situation – mechanical looseness allows much more vibration than would otherwise occur from these other problems alone.

The generation of harmonic components from sinusoidal stimuli are related to a non-linear relation between input and out of an electromechanical system – like a loudspeaker.

When a loudspeaker reproduces an audio signal, input signal and output signal should ideally be identical. If this is not the case, there is signal distortion. The Total Harmonic Distortion (THD) describes how much influence non-linear distortions have got on an originally sinusoidal alternating signal in the loudspeaker. With such a distortion, new overtones (also called harmonics) are created. A low THD is often regarded as an indicator for a good loudspeaker system. The THD metric is a good measure for the harmonics production, and the analogy between loudspeakers and motors are strait forward – it will provide a good measure for looseness.

The principle is illustrated in the following:

The **T**otal **H**armonic **D**istortion is a measurement (of the purity of the signal) of the harmonic distortion in a signal, as the ratio of the sum of the power of all harmonics to the power of the fundamental frequency.

$$THD(\omega) = \sqrt{\frac{\sum_{n=2}^{10} |Y_n(\omega)|^2}{|Y_1(\omega)|^2}} \cdot 100\%$$

Figure 38: Calculation of the Total Harmonic Distortion (THD) value, at specific frequencies w.

For a looseness application, the THD is only calculated for $\omega = RPM$.

16. Gear Analysis

The main part of rotating machines contains only of a single rotation system, but in application with the need of speed and power conversion between shafts, multiple rotating systems are introduced using gear or belt systems.

The EWA sensor algorithm portfolio contains two algorithms for gears: Spur gears (two rotating systems) and Planetary gears (three rotating systems).

The core parameter for all gears is the vibration level at the Gear Mesh Frequency (GMF). GMF is the product of the number of teeth on the gear multiplied by the running speed of the gear. It is not a fault frequency, like the four fundamental bearing frequencies, but a normal presented component in the vibration signal from a gear, as it is impossible to manufacture perfect gears (teeth profiles, concentricity, meshing characteristics etc.). When the vibration at 1x GMF and its harmonics are considered excessive, compared to normal levels or initial baseline levels, an analysis should be carried out to identify the cause of the problem. This is not only to avoid a breakdown of the gearbox, but it will increase the gear lifetime as well.

Like bearing data, gear data like tooth count are often not accessible, and only the gear factor is stated - indirectly via a nominal speed number, impacted by the slip speed.

For a Spur gear, the gear ratio and the GMF are straightforward and intuitive to calculate, as illustrated in Figure 39.

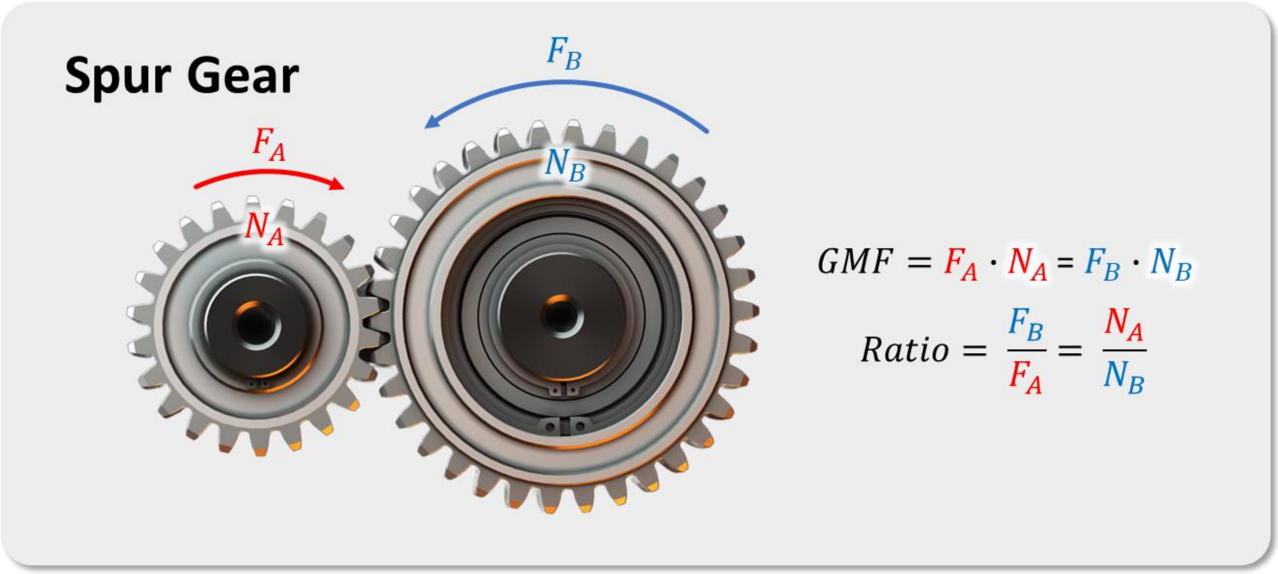

Figure 39: Spur Gear definitions.
N_A is the number of teeth for gear A, and N_B is the tooth number for gear B.
F_A is the rotating speed of gear A (in RPM or Hz), and F_B is the rotating speed of Gear B (in RPM or Hz).

In the case, that the tooth number is not provided but only the gear ratio, the following algorithm will search the vibration spectrum for a possible candidate for N_A and F_{GMF}:

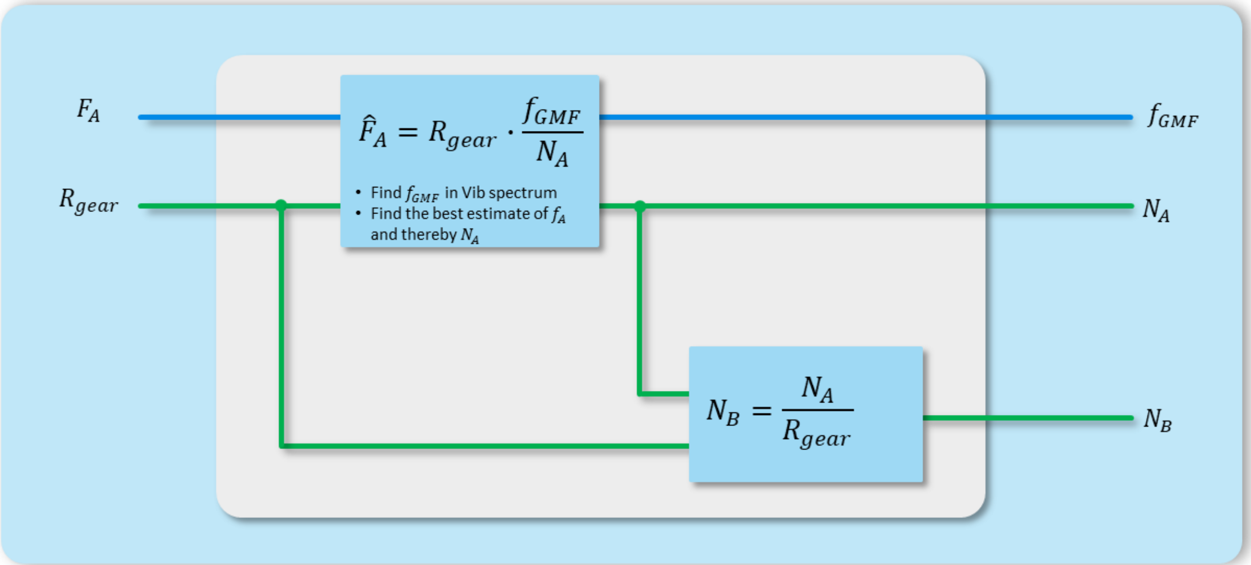

Figure 40: Calculation of the spur gear parameters N_A and N_B.

The algorithm involves the following steps:

- The gear tooth size N_A is found by searching the vibration spectra for f_{GMF} candidate, that will fulfil the following relation $\widehat{F_A} \cdot N_A = R_{gear} \cdot f_{GMF}$, where $\widehat{F_A}$ is the best estimate of F_A for the correct value of N_A.
- The second gear tooth size N_B is found using the gear ratio and N_A.

The concept of planetary gears is very different from Spur gear. As stated by the authors Arnaudov & Karaivanov of the book “Planetary Gear Grain” - *Planetary gear trains make up an extremely large technical field. The theory behind them is complex, with many unexpected challenges, while the way they function are not obvious and easy to understand. Because planetary gear trains have a reputation for being complex and hard to understand - for some, they are borderline mystical*.

When the tooth number for the sun N_s and ring gear N_r for a planetary gear are known, the corresponding gear *Ratio* and *GMF* can be directly calculated from the formulas in the following figure:

Planetary Gear

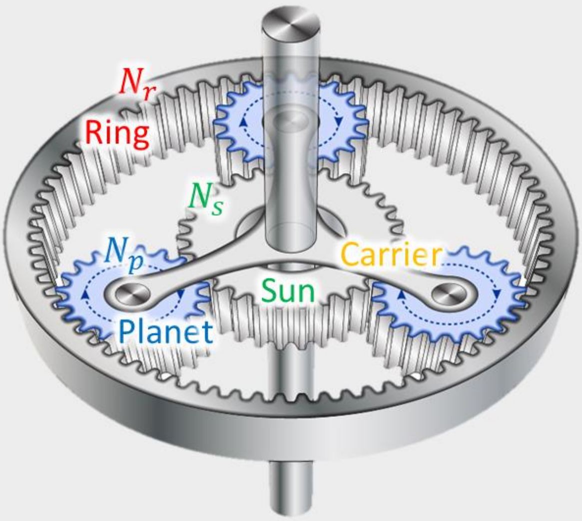

$$GMF = f_s \cdot \frac{N_s \cdot N_r}{N_s + N_r}$$

$$Ratio = 1 + \frac{N_r}{N_s}$$

Figure 41: Planetary Gear definitions.

But again, these numbers are often difficult to obtain, as most manufactures of motors are sourcing the gearbox from an external supplier and are only focused on the functionality like gear ratio and not the number of teeth. In the case, where only the gear ration and the motor RPM (M_{Rotor}) is known, the following algorithm will find the planetary gear tooth numbers, together with the gear rotation frequency, GMF:

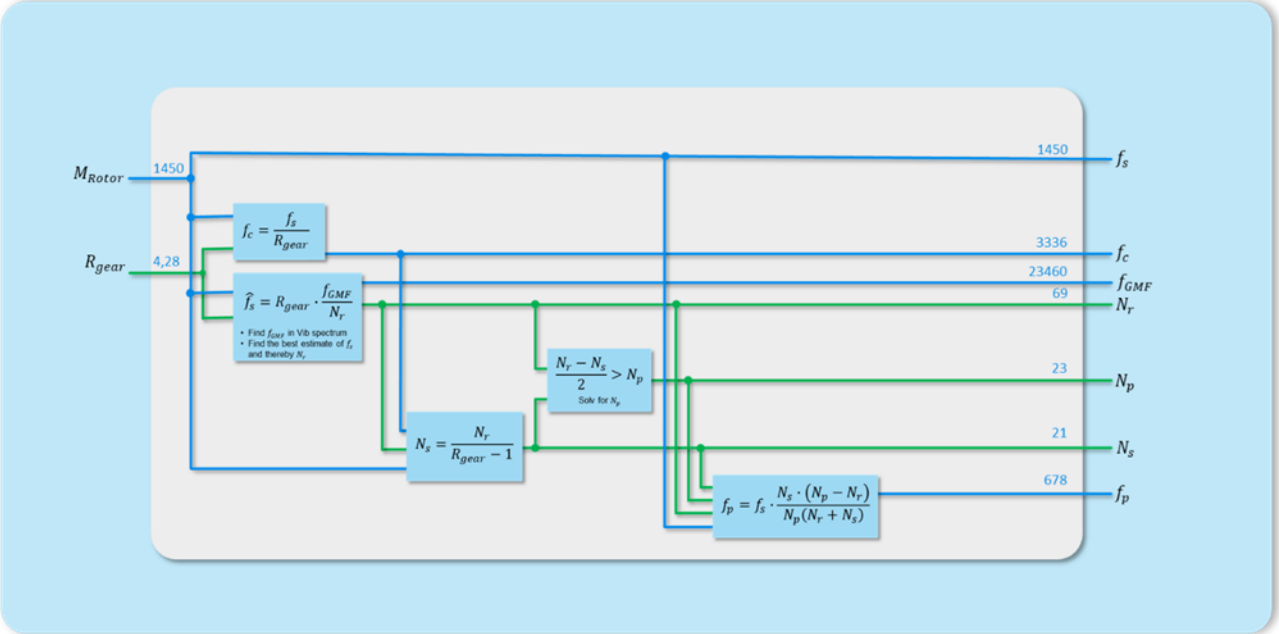

Figure 42: Planetary Gear calculation of the three individual gear tooth numbers, together with rotation frequencies. Blue example for a gear ration of 4.28 and the corresponding gear tooth numbers.

The algorithm involves the following steps:

- The Carrier rotation frequency f_c is calculated Sun rotation frequency f_s and gear ratio.
- The Ring gear tooth size $N_r$is found by searching the vibration spectra for f_{GMF} candidate, that will fulfil the following relation $\widehat{f_s} \cdot N_r = R_{gear} \cdot f_{GMF}$, where $\widehat{f_s}$ is the best estimate of f_s for the correct value of N_r.
- The Sun gear tooth size N_s is calculated from N_r and the gear ratio.
- The Planet gear tooth size N_p is calculated from the geometric constraint for planetary gears.
- The Planet rotation frequency f_p can be found from the three googh sizes and the sun rotation frequency.

Tracking and trending the GMF vibration level provides a robust measure of the gear box wear. Just to name an example of the insight, that this algorithm can provide:

> A customer was advised to reduce the rotation speed of a gear motor with 33%, from 1500 RPM to 1000 RPM to reduce the energy consumption.
>
> But the corresponding GMF vibration level increased with 200%, as the gear oil was not rated to the low speed. For this customer, what has been saved in energy, might be lost in the reduced lifetime of the gear box.

The following “collage” (Figure 43) illustrates the steps to follow, from calculating the gear tooth to the gear ratio (transmission ratio), and the GMS for the planetary gear.

Fundamental Formula for Planetary Gears

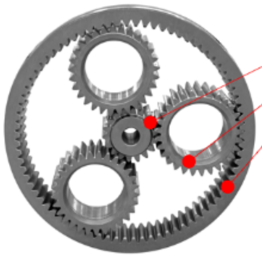

- N_s - Sun gear tooth size
- N_p - Planet gear tooth size
- N_r - Ring gear tooth size
- f_s - Sun gear rotation frequency
- f_p - Planet gear rotation frequency
- f_r - Ring gear rotation frequency

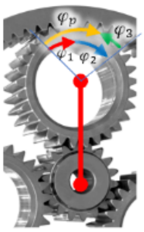

The motion of a rotating planet gear

$$\varphi_p = \varphi_{p_1} + \varphi_{p_2} + \varphi_{p_3} = \varphi_c + \frac{d_s}{d_p}\varphi_c - \frac{d_s}{d_p}\varphi_s$$

$$\varphi = 2\pi \cdot f \cdot t \Rightarrow$$

$$2\pi \cdot f_p \cdot t = 2\pi f_c \cdot t + \frac{d_s}{d_p} \cdot 2\pi \cdot f_c \cdot t - \frac{d_s}{d_p} 2\pi f_s \cdot t \Rightarrow$$

$$f_p = f_c + \frac{d_s}{d_p} f_c - \frac{d_s}{d_p} \cdot f_s \Leftrightarrow f_p \cdot d_p = f_c \cdot d_p + f_c \cdot d_s - f_s \cdot d_s \Leftrightarrow$$

$$f_p \cdot d_p = f_c \cdot (d_p + d_s) - f_s \cdot d_s$$

Willis Equation 1

$$\boxed{f_p \cdot N_p = f_c \cdot (N_p + N_s) - f_s \cdot N_s}$$

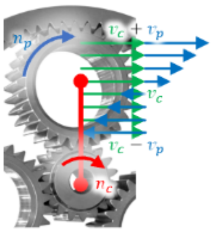

Extending Willis Equation with Ring Rotation Speed

$$\left.\begin{array}{l} V_r = V_c + V_p \\ V_s = V_c - V_p \end{array}\right\} \Rightarrow V_p = \frac{V_r - V_s}{2}, \quad V = f \cdot \pi \cdot d \Rightarrow$$

$$f_p \cdot \pi \cdot d_p = \frac{f_r \cdot \pi \cdot d_r - f_s \cdot \pi \cdot d_s}{2} \Leftrightarrow$$

$$f_p \, d_p = f_r \cdot \frac{d_r}{2} - f_s \cdot \frac{d_s}{2} \Leftrightarrow$$

$$f_p \cdot N_p = f_r \cdot \frac{N_r}{2} - f_s \cdot \frac{N_s}{2}$$

Insert into Willis first equation:

$$f_p \cdot N_p = f_r \cdot \frac{N_r}{2} - f_s \cdot \frac{N_s}{2} = f_c \cdot (N_p + N_s) - f_s \cdot N_s \Rightarrow$$

$$f_r \cdot N_r - f_s \cdot N_s = 2 \cdot f_c \cdot (N_p + N_s) - 2 \cdot f_s \cdot N_s \Leftrightarrow$$

$$f_r \cdot N_r = 2 \cdot f_c \cdot (N_p + N_s) - f_s \cdot N_s$$

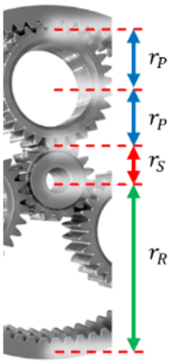

Geometric Constraint

$$N_r = N_s + 2 \cdot N_p \Rightarrow N_p = \frac{N_r - N_s}{2}$$

$$f_r \cdot N_r = 2 \cdot f_c \cdot \left(\frac{N_r - N_s}{2} + N_s\right) - f_s \cdot N_s$$

$$= f_c \cdot (N_r - N_s + 2 \cdot N_s) - f_s \cdot N_s$$

$$= f_c \cdot (N_r + N_s) - f_s \cdot N_s$$

Willis Equation 2

$$\boxed{f_r \cdot N_r = f_c \cdot (N_r + N_s) - f_s \cdot N_s}$$

Transmission Ratio

Fixed Sun gear: $f_s = 0 \Rightarrow f_r \cdot N_r = f_c \cdot (N_r + N_s) - 0 \cdot N_s \Rightarrow R_s = \frac{f_r}{f_c} = \frac{N_r + N_s}{N_r} = 1 + \frac{N_s}{N_r}$

Fixed Ring gear: $f_r = 0 \Rightarrow 0 \cdot N_r = f_c \cdot (N_r + N_s) - f_s \cdot N_s \Rightarrow R_r = \frac{f_s}{f_c} = \frac{N_r + N_s}{N_s} = 1 + \frac{N_r}{N_s}$

Fixed Carrier gear: $f_c = 0 \Rightarrow f_r \cdot N_r = 0 \cdot (N_r + N_s) - f_s \cdot N_s \Rightarrow R_c = -\frac{N_R}{N_S}$

Setup	Input	Output	Stationary	Ratio	Function	Range
A	Sun	Carrier	Ring	$1 + \frac{N_r}{N_s}$	Reduction	$1 < R < \infty$
B	Carrier	Ring	Sun	$1 + \frac{N_s}{N_r}$	Overdrive	$1 < R < 2$
C	Sun	Ring	Carrier	$-\frac{N_r}{N_s}$	-Reduction	$-\infty < R < -1$

Planetary Frequencies using Willis Equation 1+2

- Carrier Frequency

$$f_r \cdot N_r = f_c \cdot (N_r + N_s) - f_s \cdot N_s \wedge f_r = 0 \Rightarrow f_c \cdot (N_r + N_s) = f_s \cdot N_s \Rightarrow \boxed{f_c = f_s \cdot \frac{N_s}{N_s + N_r}}$$

- Planet Frequency

$$f_p \cdot N_p = f_c \cdot (N_p + N_s) - f_s \cdot N_s \wedge f_c = f_s \cdot \frac{N_s}{N_s + N_r} \Rightarrow$$

$$f_p \cdot N_p = f_s \cdot \frac{N_s}{N_s + N_r} \cdot (N_p + N_s) - f_s \cdot N_s \Rightarrow$$

$$f_p = f_s \cdot \left(\frac{N_s}{N_s + N_r} \cdot \frac{N_p + N_s}{N_p} - \frac{N_s}{N_p}\right) = f_s \cdot \left(\frac{N_s \cdot (N_p + N_s) - N_s \cdot (N_s + N_r)}{N_s + N_r}\right) \Rightarrow \boxed{f_p = f_s \cdot \frac{N_s \cdot (N_p - N_r)}{N_p \cdot (N_r + N_s)}}$$

- Gear Mesh Frequency

$$f_{GMF_{CR}} = f_c \cdot N_r = f_s \cdot \frac{N_s}{N_s + N_r} \cdot N_r \Rightarrow \boxed{f_{GMF_{CR}} = f_s \cdot \frac{N_s \cdot N_r}{N_s + N_r}}$$

$$f_{GMF_{SC}} = (f_s - f_c) \cdot N_s = \left(f_s - f_s \cdot \frac{N_s}{N_s + N_r}\right) \cdot N_s \Rightarrow \boxed{f_{GMF_{SC}} = f_s \cdot \frac{N_s \cdot N_r}{N_s + N_r}}$$

Figure 43: Planetary Gear calculations.

17. Water Hammer detection

Water hammering is a pressure surge created by a rapid change in flow velocity in a pipeline. This instantaneous change in flow velocity is often created by a sudden valve closure or pump stopping. It is the same phenomena known from signal transmission lines - an impedance mismatch in a circuit or along a transmission line will produce a reflection back to the source of the signal.

Water hammer can result from improper valve selection, in-proper valve location, and sometime poor maintenance practices. Swing check valves are prone to slamming because they rely on reversing flow and backpressure to push the disc back into the seat. If the reverse flow is forceful (as in a vertical line with flow upwards), the disc is likely to slam with great deal of force and potential damaging the casket and leading to leakage.

As Water Hammer is pressure surge of the liquid, it is not directly measurable by the EWA Sensors, as it is not in contact with the liquid through a pressure cell. But a derived effect in the form of vibration and slip speed discontinuities can be observed and used as a signature for Water Hammer detection.

An analogy for the motion of the pressure surge can be obtained from a bouncing of a ball. When dropping a ball to the floor, it will hit the floor with great force, and bounce-up again. The second time, the ball bit the floor, the force will be reduced due to conversion of initial heat/sound/impact energy to the floor and the bounce-up height will be reduced. After a couple of bounce rounds, the ball will stop bouncing. The time between impact will also be reduced after each bounce. The bouncing pattern is illustrated in the following Figure 44.

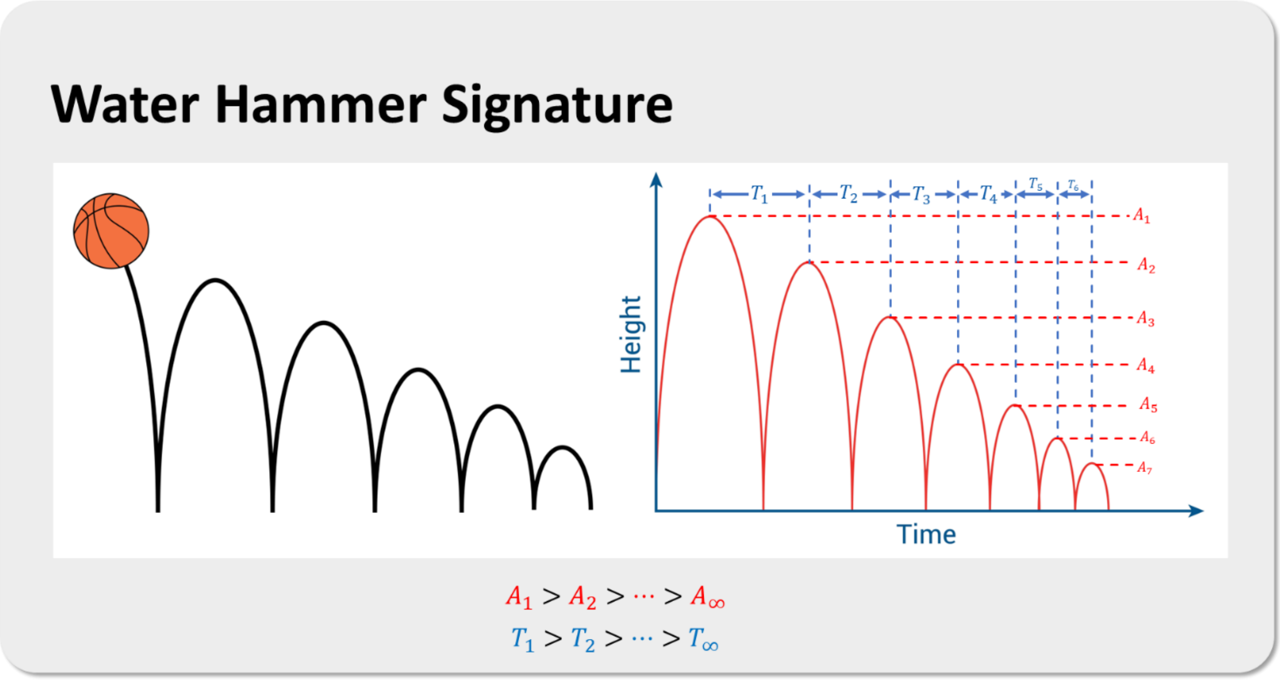

Figure 44: Illustration of bouncing pattern as Water Hammer signature.

When a large column of water is instantaneously stopped by a barrier (valve or pump), it will bounce-back like in the ball analogy. The vibration signature for a Water Hammer is:

- Time T between impacts will decrease with each bounce.
- Impact energy A will decrease with each bounce.
- Signature dataset $(T_1, A_1, T_2, A_2 \cdots)$ from Water Hammer impacts are the same for different machine installations.

It is not possible to identify a single vibration pulse as a Water Hammer incident, but multiple comparable signature datasets are a strong indicator of a Water Hammer problem. The signature dataset will be constraint by the piping, flow velocity etc., and it will be reproduceable by each Water Hammer impact. The principle drawing of the time waveform for a Water Hammer case is illustrated in the following Figure 45.

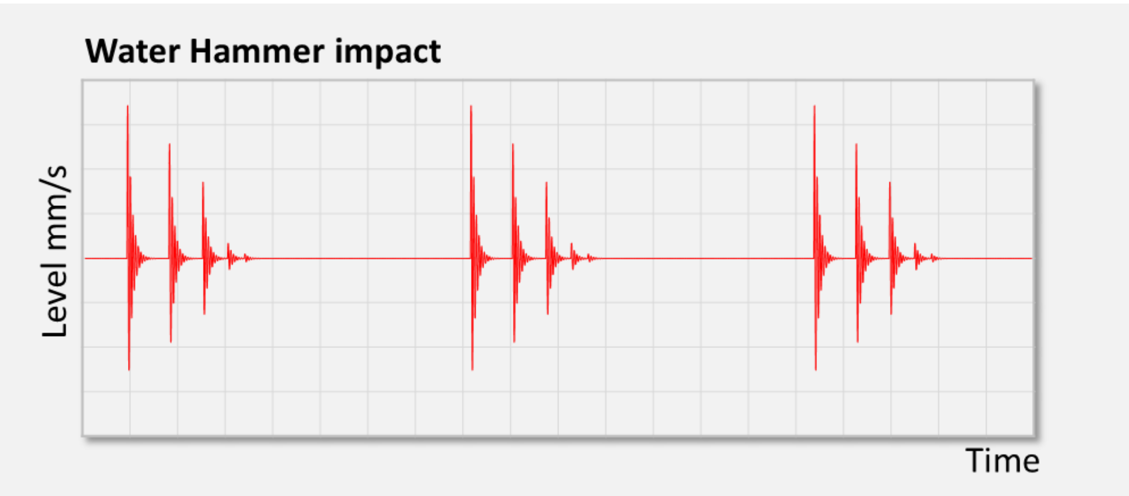

Figure 45: Water Hammer impact monitored and illustrated with the time waveform. Each impact is the impulse response of the pipe + valve + pump construction.

The Water Hammer algorithm will become available in a coming software release.

The Water Hammer algorithm has an EWA patent.

18. Machine Health

To ensure production quality and continuity, the performance of the machine becomes very important.

The performance can be inspected from both daily ***Operations Parameters*** like RPM, Unbalance, Slip Speed, Cavitation, and from ***Alarm Parameters*** like Bearing Fault Detection, and Baseline trending with warning and alarm level etc.

The daily operation parameters are used to optimize and balance production throughput without harming the machine, where the alarm parameters are used to detect abnormal level and behaviors (abnormally detection) and are more seldom in use.

This kind of parameter separation is seen in many contexts like the car dashboard: top dashboard instrumentation is for daily operation (speed, temperature, fuel level), and the bottom instrumentation are alarm parameters (check-engine light, Coolant Temperature light, Transmission Temperature). When driving a car, we inspect the ”daily parameters” to insure and follow the expected operation, and we don’t pay attention to alarm parameters not appearing. But when one of the car alarms appears, it is often a very serious problem and costly to repair.

Figure 46: Instrument panel (dashboard) in a car, with operation parameters and alarm parameters.

Vibration analysis is used to monitor the condition of rotating equipment and predict machine issues based on data trends over time, abnormal frequencies, or the amplitude of the measured vibration.

The first step to a successful vibration analysis is establishing relevant baseline references and alarm levels, as to help identifying when the machine is operating normally and when there is a fault/operation issue.

Vibration analysts typically use a couple of the following five reference methods to quantity and severity evaluate a machine installation:

1. Baseline readings from the installation time.
2. Generic severity charts from ISO, ANSI etc.
3. Equipment manufacturer's recommendation.
4. Statistical Data analysis from a large population of the same type of machinery.
5. Experience.

The EWA sensor is using a baseline approach. In classical vibration analysis, baselines are established by measuring the vibration of a machine when it is in good condition. The initial vibration levels at the sensor installation is recorded and used as a reference point for future measurements. By comparing the current vibration levels to the established baselines, maintenance personnel can identify trends indicating changes in a machine behavior. This information can be used to predict when a machine is likely to fail, allowing for proactive maintenance.

A static fixed-value baseline approach has some practical challenges:

- Choosing the correct time to make the baseline measurement (considering machine loads, seasonal variations over winter and summer etc.). It the baseline is set too low, it will provide false alarm, and is the baseline set too high, it will make the system blind.
- Drift of parameters related to aging and normal wear.
- New baselines are required after each machine overhaul and major service.

Regarding warning and alarm levels, it is generally believed that in the absence of other specific information a doubling of an acceptable vibration level is an indicator of trouble, and a tripling of the level is cause for major concern. The factor setting of 2 for warning level and a factor of 3 for alarm level are completely aligned with the levels given by the ISO 20816 generic severity chart.

The principle of using a static Baseline level (B) with a corresponding static warning level (2·B) and static alarm level (3·B) is illustrated in the following graph in Figure 48.

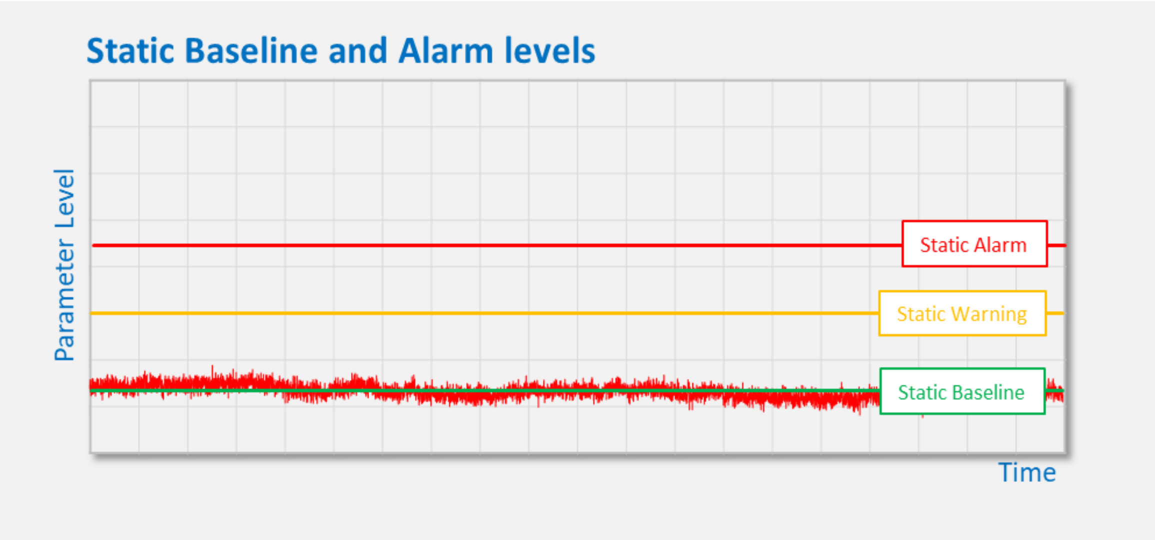

Figure 48: Illustration of monitoring data (red graph), added a static baseline and static warning and alarm limits.

Parameter levels for Vibration RMS, Unbalance etc. for a new machine will drift over time because of machine aging and normal wear. With a static setup, a machine parameter can drift into a warning or alarm situation over a year, even for a machine without any severe faults (just due to normal wear and tear). This is illustrated below.

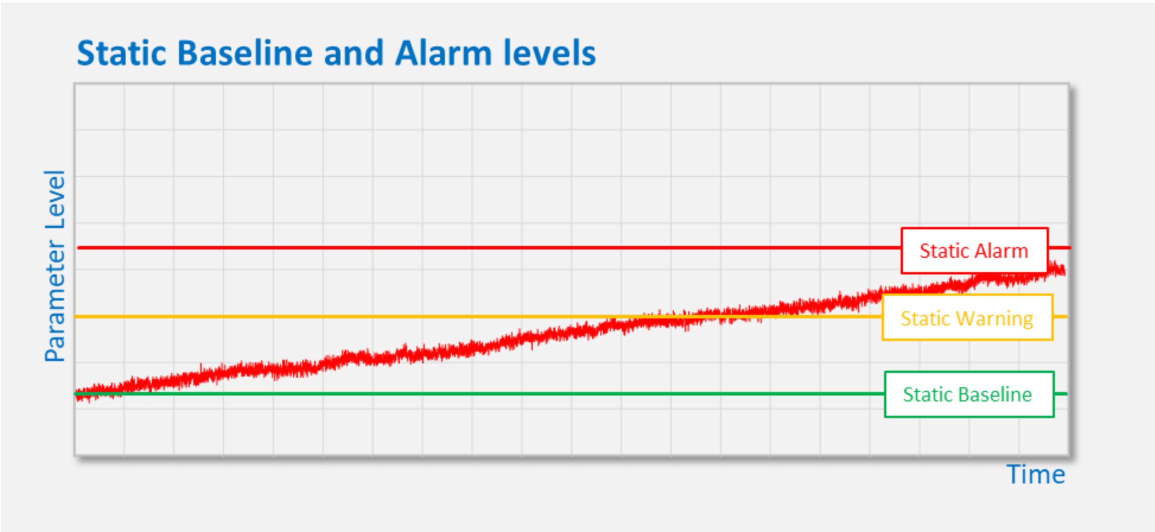

Figure 47: Illustration of the development in a monitored parameter over time (red graph), due to machine ageing and wear.

The static baseline is a measure of the parameter level from a new machine. It can be an advantage to update this level continuously, to counter-act machine wear and to obtain a baseline aligned with the aging of the machine.

The EWA sensor is based on a Dynamic Baseline approach. The dynamic EWA parameter baseline is designed as an adaptive filter, that tracks the behavior of the individual sensor parameter, in a rigid and slow manner. The principle is illustrated in Figure 50 and Figure 49.

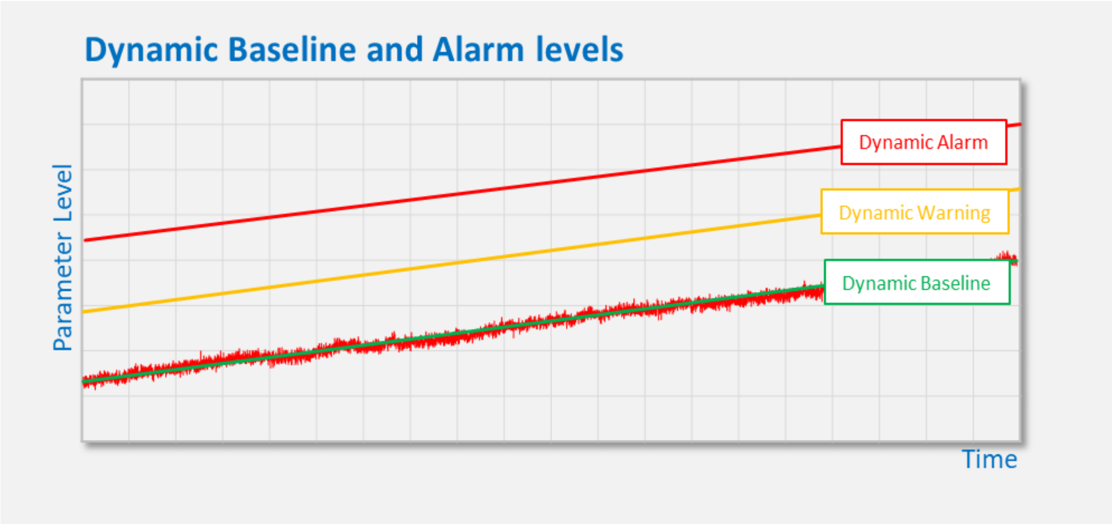

Figure 50: Illustration of a monitored parameter (red graph) using a dynamic baseline, with corresponding dynamic warning and dynamic alarm limits.

The dynamic baseline is slow, and it will not adapt to small local variations in the parameters:

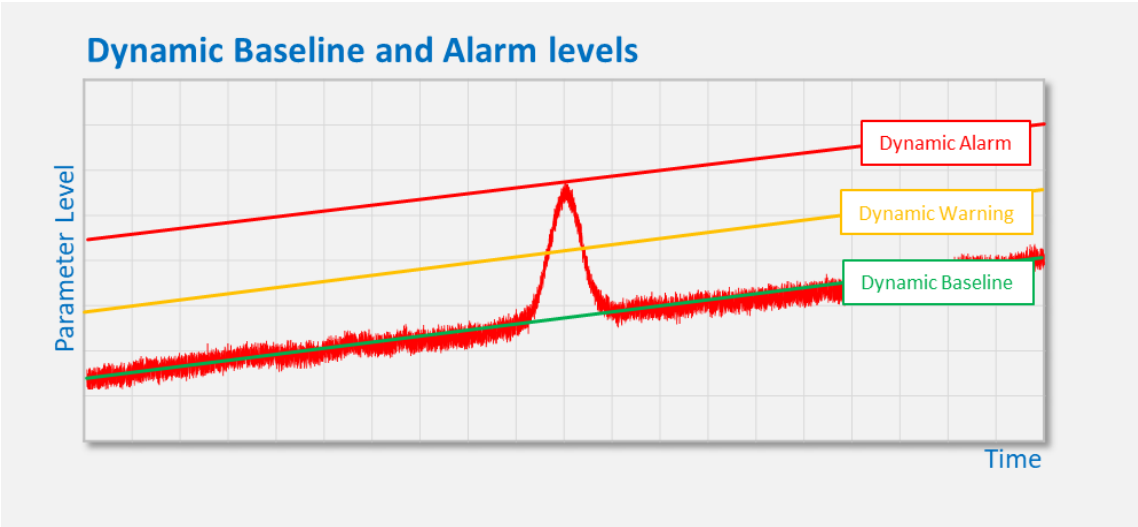

Figure 49: Illustration of a monitored parameter signal with sudden evidence (red graph), using dynamic baseline with dynamic warning- and alarm limits.

The advantage of using a dynamic baseline approach, where the baseline is adapting rigid and slowly to the measured parameter, is a flexible solution for an edge-based standalone sensor. Just to name some points:

- The baseline will adapt to normal machine aging and wear.
- Baseline tracking can be activated at the time of installation, and any deviation related to wrong timing will slowly be corrected within a week.
- New parameter levels due to a service visit will automatically initiate an adjustment of the baseline.

As a last line of defense, a static Alarm level is defined as four times the baseline. The static alarm ($B_{Initial}$) is generated after 4 hours of machine operation.

From the above definitions, the EWA sensor operates with 1 warning and 2 alarm levels, defined by:

- Dynamic Warning Level $= 2 \cdot B$
- Dynamic Alarm Level $= 3 \cdot B$
- Static Alarm Level $= 4 \cdot B_{Initial}$

The principle is illustrated in the following figure:

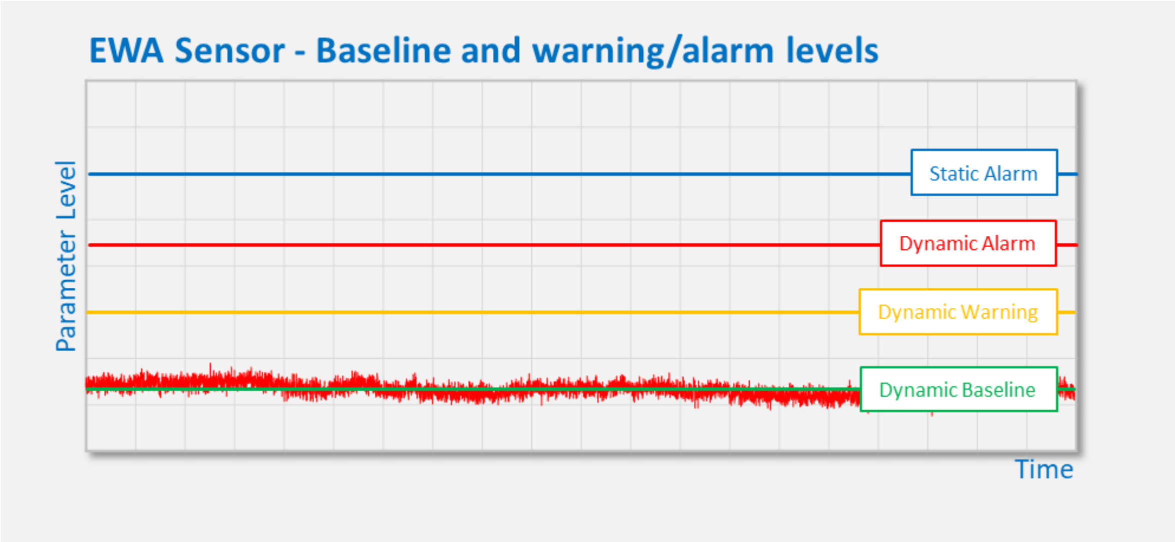

Figure 51: Illustration of dynamic baseline and dynamic warning/alarm levels, added a static alarm.

The initial baseline value ($B_{Initial}$) recorded at the time of installation, can also provide valuable insight and knowledge about the single parameter relative to its time of installation:

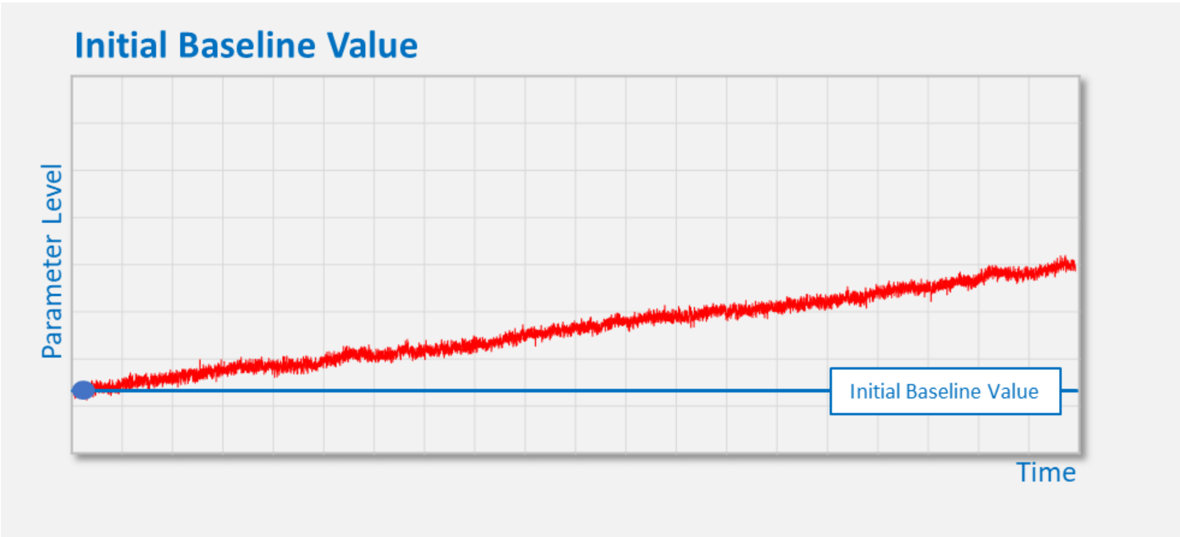

Figure 52: Illustration of the Initial Baseline plotted together with a parameter data, plotted over a certain operation time.

The EWA Sensors algorithm for Machine Health is founded on the concept of dynamic baseline tracking with belonging dynamic warning/alarm levels.

When the sensor has just been installed, it has no information regarding normal and high parameter levels, as this requires:

- information about machine size - is this a 2kW motor or an 25kW motor?
- information about machine wear history - is this a new installation or an old installation?
- information about previous failure history - is the machine already in severe unbalance?

In general, this information is not available for most installations and would be difficult to obtain, as every machine is different in respect of piping, foundation, application - all are impacting the machine operation.

The EWA sensor is designed as a ”plug and play” sensor with no initial setup or application configuration. The sensor will auto-detect the actual machine orientation (Horizontal or Vertical) and the Motor Pole Pair number. When all the auto-detected values are regarded as “good”, the sensor will be powered on, and the parameter baselines will adapt to current monitored parameters values within 12 hours of machine operation.

The EWA sensor is automatically generating baselines for 8 parameters, see Figure 53 (more parameters will follow in future):

- Unbalance
- Bearing Fault Detection
- Cavitation
- Temperature
- Vibration RMS X-axis
- Vibration RMS Y-axis
- Vibration RMS Z-axis
- Gear Mesh Frequency

When a measured parameter crosses any of the three levels for more than 10s, a corresponding flag is raised at the Machine Health center. The flag is automatically put down again after one hour with no warning/alarm occurring.

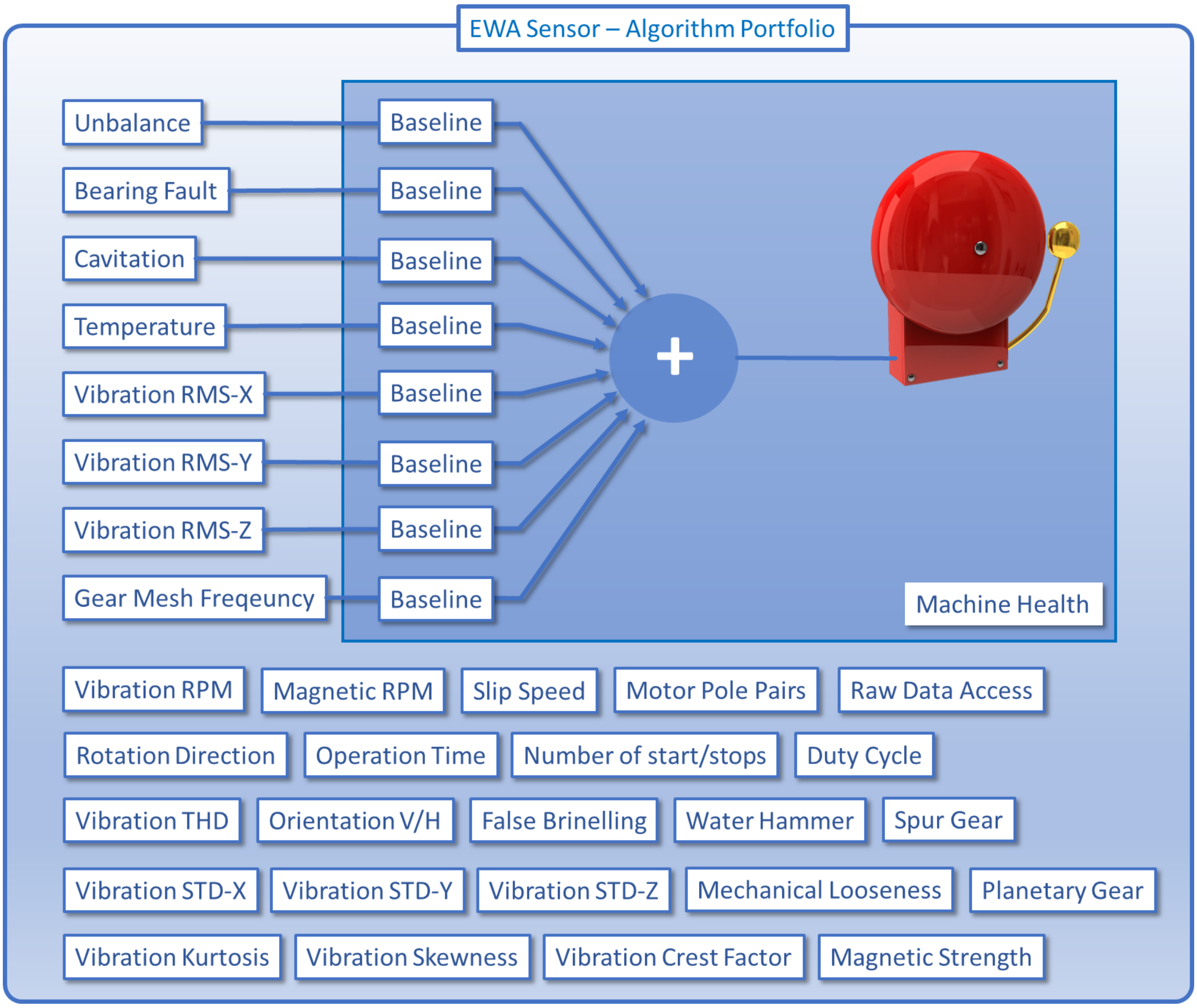

Figure 53: The EWA Algorithm Portfolio consists of fault parameters with their individual calculated dynamic baseline, and operation parameters and development parameters without baselines.

The Health Center algorithm will indicate the highest severity level, both as a status on the Modbus and indicated on the Alarm LED on the front of the EWA Sensor, see Figure 54.

After sensor power-on, the sensor will use around 12 hours to build-up the baselines. During this time, the Health Center will be inactivated, as it will not able to make any assessments without baselines.

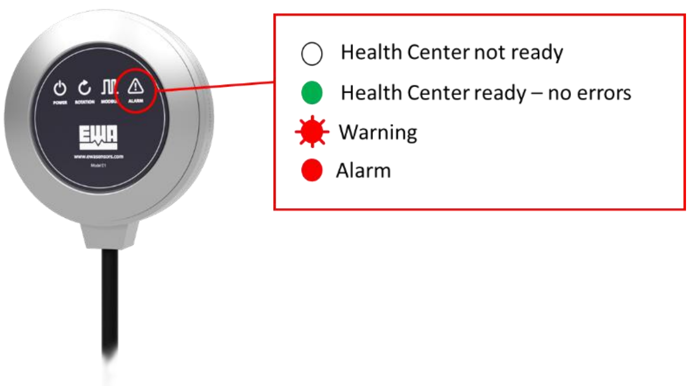

Figure 54: Sensor LED indications for status of the Health Center.

The graph below illustrates a real-life example for monitored vibration RMS with baseline and alarm / warning levels:

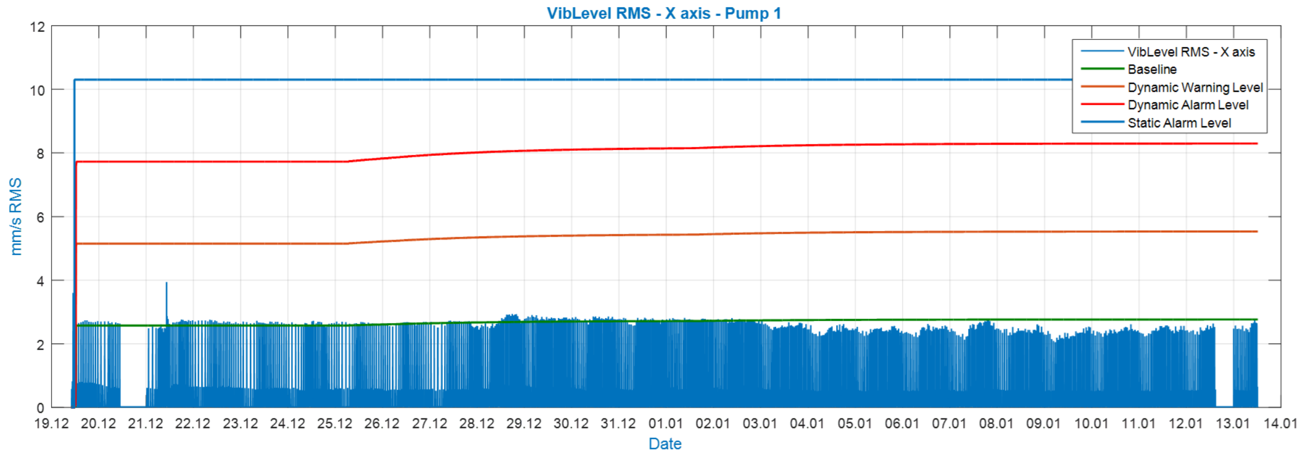

Figure 55: Baseline calculation for the vibration RMS parameter, for a pump installation. The calculated dynamic warning and alarm limits are also plotted.

Currently, 8 parameters are tracked with baseline and alarm levels. When a parameter crosses a warning or alarm level, the Health Status flag for the parameter will be updated with the value 2 (warning) or 3 (alarm). If the Health Status for a parameter persists for more than 10 seconds, the health status flag will be transmitted to the Machine Health. The Machine Health algorithm will maintain the Health status for a period of one hour, after the Health Status flag has been cleared. This illustrated in the following graph:

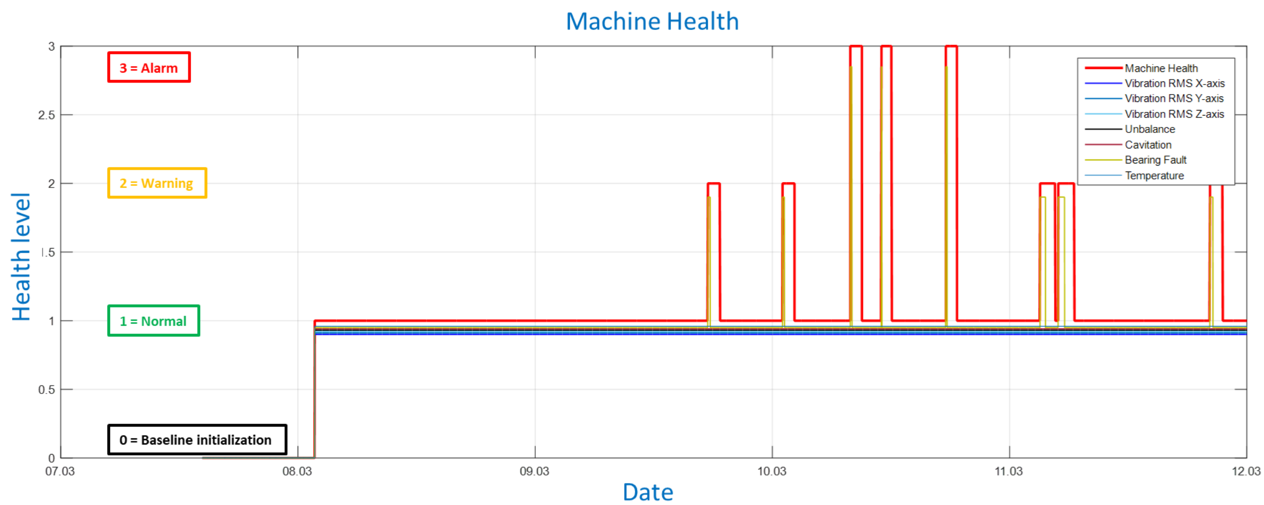

Figure 56: Monitored signal for Machine Health, showing both Normal condition (1=Normal), Warning condition (2=Warning) and Alarm condition (3=Alarm). When the Machine Health flag has been set, it will keep the Health status for one hour after the flag has been cleared.

Figure 56 illustrates the Machine Health and the corresponding 8 parameter Health Status. The 8 Health Status parameters are displayed with an offset, to avoid overlapping graphs. The EWA sensor starts with a 12 hours initialization period to build the baselines. After two days of operation, the bearing algorithm sets the Health Status flag, to signal a warning issue. This is later upgraded to an alarm issue.

The EWA Health Monitoring and the dynamic approach has an EWA patent pending.

19. ISO 18436 Compliance

Condition monitoring of rotation machinery has become so mature, that the International Organization for Standardization (aka ISO) has defined a dedicated certification standard ISO-18436, that specifies requirements for the training, relevant experience, and examination of personnel performing condition monitoring and diagnostics of machines using vibration analysis. The standard's part 2 of this ISO certification "*Vibration condition monitoring and diagnostics*" are divided into four classification categories, from Cat I: *Introduction Level* to the Cat IV: *Advanced Level*.

The benefit of a certification standard within condition monitoring is to outline best practice for condition monitoring for rotation machinery, covering every aspect from sensor design to how to measure and interpret vibration data. When being in compliance with ISO-18436, all professionals are "talking the same language", and measurement methods are comparable and aligned.

EWA Sensors has selected to build the sensor platform on this huge foundation of knowledge and has therefore attended all certifications (Cat I to Cat IV) from the three leading certification institutes: Mobius Institute, Technical Associates of Charlotte and Vibration Institute.

Figure 57: The three main providers of ISO 18436-2 certifications.

By following the 12 sections (Cat I to Cat IV from these three institutes) a solid state-of-the-art foundation has been built, to guide the design of an innovative sensor platform and algorithm portfolio for the EWA sensor.

Figure 58: The EWA Sensors has achieved ISO 18436-2 certifications CAT IV from Technical Associates and Mobius Institute, and CAT III from Vibration Institute.

Figure 59: Route-based monitoring on a dry-installed wastewater pump.

20. Remote Firmware Upgrade

The benefit of edge processing is fast and local processing of data, as the algorithms are running in a local target.

To keep the algorithm portfolio of an EWA sensor up-to-date, and enable remote sensor updating with new parameters, the EWA sensor firmware can be updated over the Modbus.

Currently, there are two approaches for sensor firmware updating:

- PC software from EWA Sensors, connecting the sensor Modbus network to a PC using a USB converter, and updating sensors using the EWA Bootloader PC program.

  Individual EWA sensors on the network can be addressed and updated – one at a time. Details can be found in the pdf document *EWA PC Bootloader Use Guide*.
- Customer implementation of the update procedure in gateway, PLC or SCADA – following the EWA software guide for updating the sensor. Details can be found in the pdf document *EWA Bootloader Protocol Specification*.

Both approached are supported by two pdf documents.

Firmware updating of an EWA sensor takes approximately 55 sec. per sensor. The following figure illustrates a firmware update using the PC software. The current version is through a PowerShell window or a windows command prompt, but a pure Window version will soon be available.

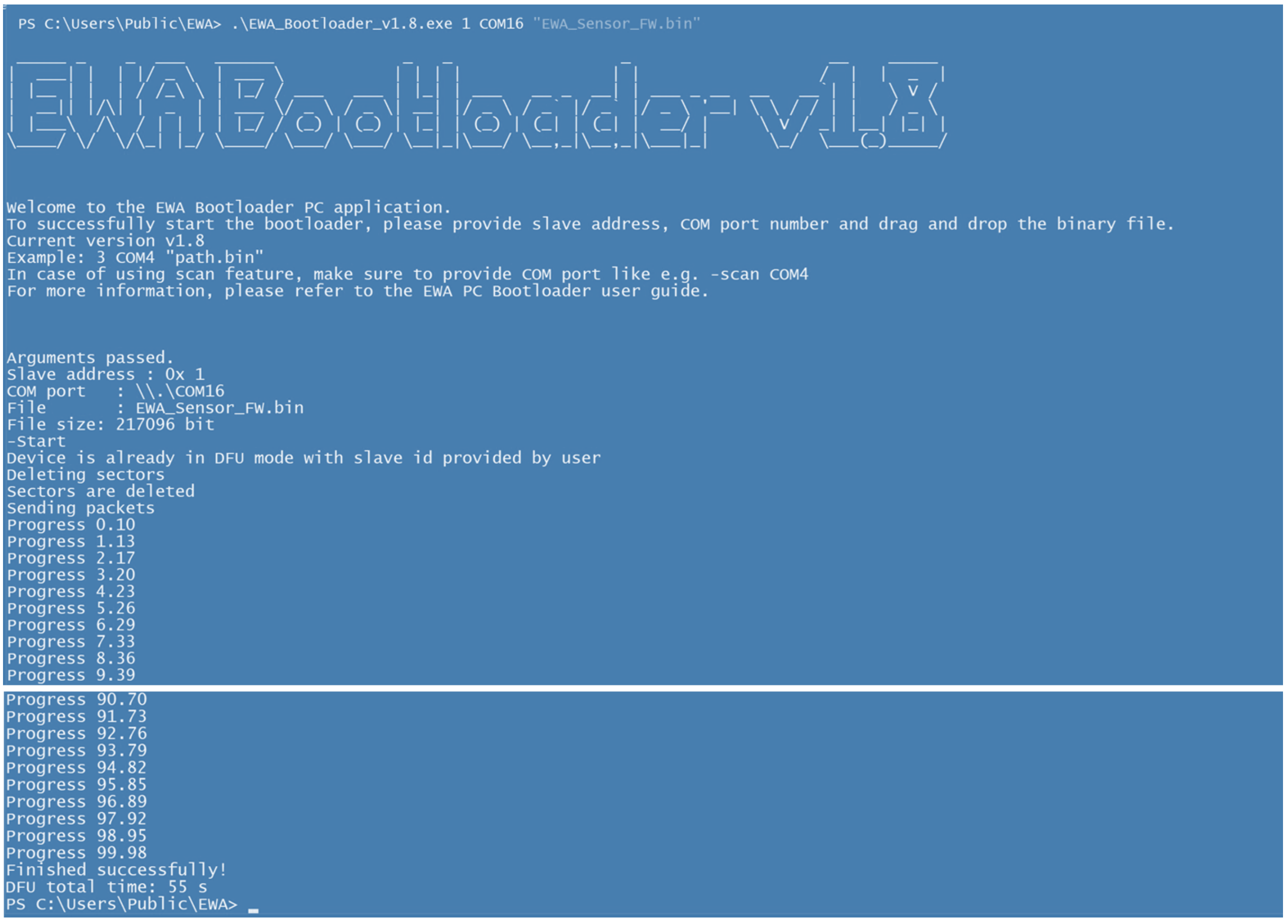

Figure 60: Firmware updating, using the EWA PC bootloader software.

21. Raw Data access

The EWA sensor is an Edge Device, where all signal analytic are performed by an embedded powerful microcontroller, and the resulting parameters are accessible using Modbus.

Moving all raw sensor data to a cloud platform will be both technical challenging (continuously streaming of 6 channels with 32kHz bandwidth and 16bits data) and expensive in data cost. An edge solution is a more elegant and green solution, as data stay at the source and are processed locally by a low-power processing unit. The technical requirement for communicating with an edge solution is easily obtained through the Modbus fieldbus (as used in many customer installations).

In three cases, the access to raw data become mandatory, also for an edge device like the EWA sensor:

- Foundation for developing new sensor algorithms and parameters.
- Manual data inspection.
- AI and ML support

To fulfill this need, the EWA sensor is providing continuous access to 2 seconds of both vibration and magnetic raw data with a sampling frequency of 2kHz. Five Modbus registers are used for this: two registers for a floating-point vibration sample, two registers for a floating-point magnetic sample and one register for indexing. A coherent sample set for vibration, magnetic and index are obtained during every block transfer of the parameter list, and a complete 2 sec. data set are thereby obtained approximately every hour, at no extra cost.

The indexing is included with each Modbus reading. In many cases, the raw data will be an extra bonus, to be used when going back to inspect historical data. To decrease the time to retrieve a complete dataset, a dedicated block transfer only of the five Modbus registers with raw data can be made - but this will block for the normally communication on the remaining Modbus protocol.

The retrieval of raw data is illustrated in the following graph. The first plot shows the consecutive reading of the parameters for a duration of 24 hours. This track contains approximately 20 complete raw data sets. Subsequently, the raw data for the first running pump operation cycle at 8am is extracted at the bottom plot.

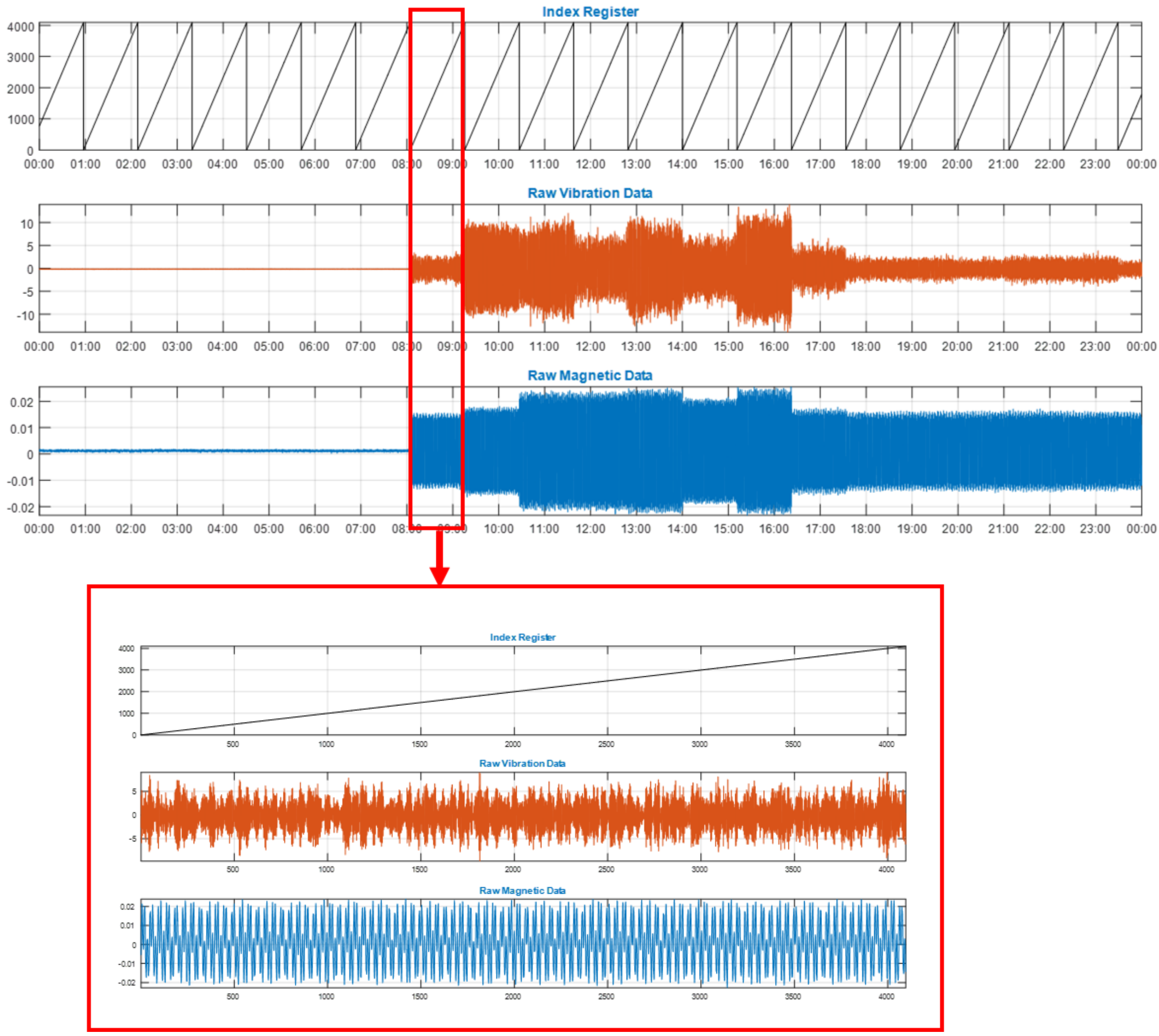

Figure 61: Upper plot shows associated values of indexing, raw vibration data and raw magnetic field data for a 24-hour operation period. The lower plot is an extraction of 2 seconds of data from the upper plot, for a pump running sequence started at 8am.

The EWA sensor is a multi-rate platform using sampling frequencies of 2kHz, 8kHz and 32kHz. Currently, the raw data access is provided to the 2kHz domain, but access can easily be extended to both 8kHz and 32kHz, if needed.

22. Customized algorithm design.

The EWA sensor is a powerful edge device with an internal 480MHz Cortex-M7 microcontroller for signal analytics. The current load of the microcontroller is only 50%, so the platform is capable of running more algorithms.

EWA Sensors are therefore offering customers to develop customized solutions, tailor-made to specific machinery and applications, that are not covered by the current algorithm portfolio. The EWA sensor is a multi-rate platform with sensor data in both 2kHz, 8kHz and 32kHz format, for both 3D vibration and 3D magnetic signals.

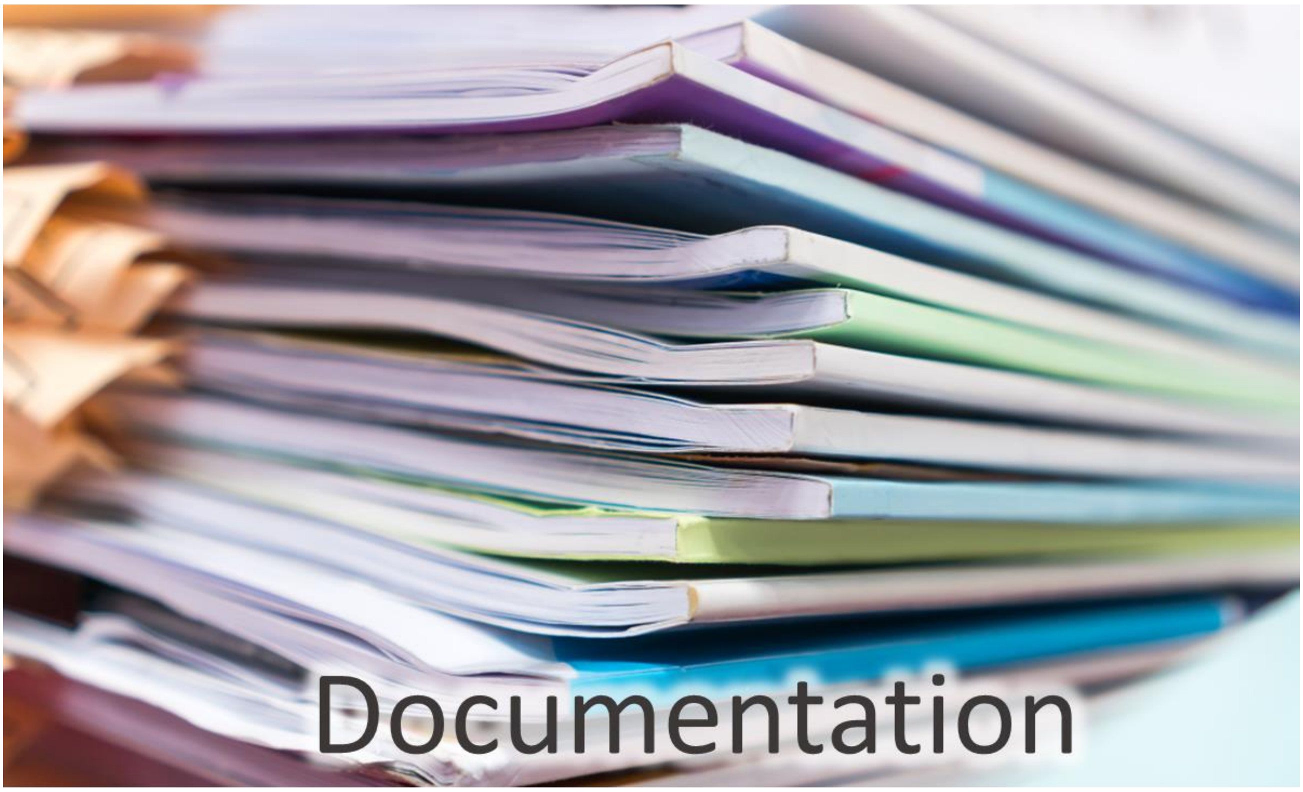

23. Technical sensor documentation.

The EWA sensor is documented and supported in following technical documents:

1) One-Pager
2) Datasheet
3) User Manual
4) Modbus Interfacing Guide
5) PC Bootloader Use Guide
6) Bootloader Protocol Specification
7) Whitepaper, "EWA sensors for Condition Monitoring on Rotating Machinery"

Figure 62: Technical documentation, for the EWA sensor.

ABOUT EWA Sensors:

EWA Sensors is a Danish company, developing and manufacturing edge-based sensors for condition monitoring and predictive maintenance of rotating machinery. EWA Sensors core capabilities lay in high-quality sensor signals and in advanced algorithm design.

Algorithms, both for edge-based and cloud-based solutions, are not better than the data quality they are fed with. EWA has focus on the sensor monitoring circuits, to secure high-quality data and the required signal bandwidth for algorithm development.

All EWA signal processing and algorithm designs are based on signature design in time domain and in frequency domain. Furthermore, algorithm design use combination of signals in one-, two- or three dimensions (x-, y- and z-dimension), to secure robust and strong parameter estimation, and for new signatures and parameter designs for the future.

On top of the algorithm design is added an Early Warning Analytics (EWA) layer, making a clear and easy to understand evaluation on each single sensor parameter.